

Inferring average generation via division-linked labeling

Tom S. Weber*, Leïla Perié† and Ken R. Duffy‡

3rd June 2015

Abstract

For proliferating cells subject to both division and death, how can one estimate the average generation number of the living population without continuous observation or a division-diluting dye? In this paper we provide a method for cell systems such that at each division there is an unlikely, heritable one-way label change that has no impact other than to serve as a distinguishing marker. If the probability of label change per cell generation can be determined and the proportion of labeled cells at a given time point can be measured, we establish that the average generation number of living cells can be estimated. Crucially, the estimator does not depend on knowledge of the statistics of cell cycle, death rates or total cell numbers. We validate the estimator and illustrate its features through comparison with published data and physiologically parameterized stochastic simulations, using it to suggest new experimental designs.

1 Introduction

Given a proliferating population of cells starting from one or more progenitors, a natural quantity of interest in cell biology is the average number of divisions per cell since the initial progenitors, i.e. the average generation of presently living cells. The average generation is related to the population's turn-over rate and can potentially be used to quantify dynamics and aging of the immune system [69, 28, 9, 40], to better understand the evolution and risk of cancer [15, 42, 66], and to rank cell types in hierarchies of complex differentiation programs [25, 73].

Estimating average generation is a simple matter if cell lifetimes are all equal and the division time is known or, alternatively, if total cell counts can be measured and there is no cell death. If, however, lifetimes are heterogeneous, the population is subject to death as well as division or total cell counts are not available, the issue is more involved. In these settings, several experimental techniques can be employed to estimate average generation, including time lapse microscopy, division diluting fluorescent dyes, and inference from somatic mutations and telomere length.

The most unambiguous measurement technique is *in vitro* time lapse microscopy as it affords nearly direct determination of lineage trees and cell generation. Time lapse microscopy has been used to

*Hamilton Institute, Maynooth University, Ireland

†Division of Immunology, Netherlands Cancer Institute & Theoretical Biology and Bioinformatics, Utrecht University, the Netherlands. Present address: Curie Institute, CNRS UMR 168, Paris, France.

‡Hamilton Institute, Maynooth University, Ireland. E-mail: Corresponding ken.duffy@nuim.ie

study many cell systems including bacteria, lymphocytes, embryonic development, gut development, to name but a few, e.g. [48, 60, 63, 24, 61, 41, 20, 13, 18, 52, 10]. Even it, however, has limitations as filming is not continuous, cells can leave the field of vision or form three dimensional structures that inhibit tracking. The complexity of image segmentation increases with cell numbers, and so time lapse microscopy has proved challenging if more than approximately 10 generations are to be followed.

Another popular experimental approach, particularly in immunology, is to stain starting cells with a fluorescent dye such as Carboxyfluorescein Succinimidyl Ester [39, 38, 23], CellTraceTM Violet or Cell Proliferation Dye eFluor 670 [49]. With each division, cells inherit approximately half of their parent’s dye and so fluoresce with half their intensity. A cell’s generation can thus be determined by its luminous intensity via flow cytometry. This approach is used both *in vitro* and *in vivo*, and allows the experimenter to start with a large number of progenitors without difficulty. It enables 6-10 generations to be followed before dye dilution is such that the signal-to-noise ratio is too high for a cell’s generation to be reliably determined.

Determining generation *in vivo* remains challenging as often it cannot be achieved by direct observation or cell stain methods. Estimating replicative history, cell depth and lineage trees has been proposed by measurement of average telomere length [21, 1, 68, 72, 53, 25] or by the number of somatic mutations, which are introduced during DNA duplication [57, 67, 58, 70, 50, 7]. While methods in this direction rely on inference rather than direct observation, they offer the possibility of tracing more than 10 generations in a wide range of species, including humans.

In the present paper, we provide a novel average generation estimator that is designed with the *in vivo* setting in mind. The estimator is suitable for systems where cells undergo an unlikely, heritable division-linked label change with a determinable probability, where the label serves only as a marker and does not impact on cell dynamics. Chief amongst the estimator’s desirable properties are that: (1) it requires no information on cell lifetime distributions; (2) the population can be subject to death as well as division; and (3) only a proportion of label-positive to total cells needs to be measured. The present article introduces the estimator, analytically establishes its fundamental properties, validates its applicability by comparison with simulation and comparison with published data, proposes an experimental realization, and demonstrates its utility.

In Section 2 we describe the estimator and explain how it can be used. The estimator appropriateness is a consequence of theorems that are presented in detail in Section 4, with a heuristic explanation and overview of them appearing first in Section 3.

In Section 5, Validation Using Simulated Data, we use Monte Carlo simulations to assess the estimator’s performance for physiological parameterizations. In Section 6, Validation Using Published Data, we use several sources of publicly available data to illustrate the estimator’s applicability. We avail of complete lineage tree data for the development of *C. elegans*, as determined from time-lapse microscopy [52], stochastically labeling it. Applying the estimator results in accurate inference of the average generation in comparison to the directly observed quantity. We also take data from two distinct experimental studies, one on human colorectal cancer cells [16] and one on murine embryonic fibroblasts [32], that employ micro-satellite mutation fluorescent reporter systems. Micro-satellite mutation is an unlikely division linked change and the fluorescence of cells in these systems serves as a label suitable for average generation estimation. The results show consistency between average generation estimates, measured quantities and values reported in the literature.

As an illustrative example, in Section 7, Experiment Design, we propose a genetic construct, based on existing pieces, to facilitate average generation inference. We describe how the probability of label-loss

could be measured and how the method could be validated. In Section 8, Discussion, we conclude with experimental designs where the method would prove biologically informative.

2 Estimator Overview

We consider a system where cells are subject to a division-linked, heritable label change that serves as a measurable distinguishing marker, but does not influence population dynamics. The method is appropriate regardless of whether initial cells are label-negative and can gain the label, which is then inherited by their offspring, or are label-positive and can lose the label, with their offspring not regaining the label. For a consistent description, we phrase the paper in terms of the latter, but the results all hold *mutatis mutandis*.

During each cell's lifetime, assume that a label-positive cell becomes label-negative with a known, small likelihood, p . Let $Z(t)$ be the total live cell count at time t and $Z^+(t)$ be the live cell count of label-positive cells. Assume that the initial cells at $t = 0$ are all label-positive and that at some time t the fraction of label positive cells to total cells, $Z^+(t)/Z(t)$, can be measured. With $G(t)$ denoting the sum of the generations of all cells living at time t and with $G(0)$ defined to be 0, then given there are label-positive cells in the system at t , i.e. $Z^+(t) > 0$, we establish that the average generation of cells alive at time t satisfies the following relationship

$$\frac{G(t)}{Z(t)} \approx -\frac{1}{p} \log \left(\frac{Z^+(t)}{Z(t)} \right). \quad (1)$$

That is, the average generation of the population can be estimated directly from the proportion of label-positive cells if the delabeling probability is known.

Perhaps unexpectedly the formula (1) does not depend on several difficult-to-measure factors such as cell-lifetime distributions and total cell counts. Moreover the right hand side of (1) requires only a proportional measurement of label-positive cells, which can be determined from a sample, and the relationship holds even though the population could be subject to death as well as division.

For the validity of (1), we have assumed that at $t = 0$ all cells are label-positive. As a result $Z^+(0) = Z(0)$ and so both the right and left hand side of (1) are 0 at $t = 0$, agreeing irrespective of the initial starting number. If, however, not all cells are initially label-positive, the estimator and the average generation would not agree. This can be rectified if measurements of the proportion of positively labeled cells are available at two time-points, $t_2 > t_1$. Then, irrespective of the initial composition of label-positive and label-negative cells, so long as $Z^+(t_2) > 0$,

$$\frac{G(t)}{Z(t)} \approx \left(\frac{t}{t_2 - t_1} \right) \left(-\frac{1}{p} \log \left(\frac{Z^+(t_2)Z(t_1)}{Z^+(t_1)Z(t_2)} \right) \right). \quad (2)$$

This two-measurement estimator has an additional advantage when initial cell numbers are small. If the culture is started, as an extreme example, with a single progenitor, then the right hand side of (1) can be subject to stochastic fluctuations at shorter time-scales (see the Monte Carlo simulations in Section 5). As established rigorously in Section 4, with $t_1 > 0$, the two-sample estimator in (2) is more accurate than (1) as it removes the influence of the timing of early cell events on the estimate.

3 Explanation of the Estimator's Origin

The estimators (1) and (2) have non-obvious forms. Utilising expansion properties of cumulant generating functions, results in the following section show that the relationships hold, in expectation, for an arbitrary familial relationship. This includes, in particular, estimation of average generation for heterogeneous cell populations with distinct, potentially interdependent, proliferation characteristics.

In the absence of a generative model of family trees, however, that derivation cannot provide information about the development in time of the average generation of a family of cells. Nor can it be used to determine time-dependent properties of the estimators on a developing population. For a more detailed analysis of sample-path, multi-progenitor and time-dependent properties, a general mathematical framework for capturing the stochastic dynamics of a proliferating cell system subject to division and death, as well as heterogeneous cell life times, is that of age dependent branching processes [22, 29] where cells have random lifetimes as well as random numbers of offspring. Since the seminal work of Bellman and Harris [5], it has been known that if cells are more likely to divide than die, given the cell population does not die out, the number of cells living at time t grows exponentially in time, $Z(t) \sim \exp(\alpha t)$, at a rate, α , dubbed the Malthus parameter, that depends on the lifetime and offspring number distributions of cells. This result is known to be robust, for example, to sibling dependencies [8, 46, 12].

In a cell system experiencing heritable one-way label-changes, label-positive cells can become label negative-cells, but the reverse is not possible. Thus the number of label-positive cells at time t also satisfies the branching process result, $Z^+(t) \sim \exp(\alpha^+ t)$, but with a Malthus parameter that is smaller than that for the total label-independent population of cells, $\alpha^+ < \alpha$. The difference $\alpha - \alpha^+$ depends on the likelihood, p , that a label-positive cell loses its label.

Fewer results have been established regarding the total generation of a cell population, the sum of the generations of all cells living at time t , $G(t)$, for which new theorems can be found in Section 4. For the label-independent population, in substantial generality we prove that $G(t) \sim t \exp(\alpha t)$. That is, the total generation increases faster than the total population size by a factor of t . Recalling that $Z(t) \sim \exp(\alpha t)$, for a general age-dependent branching process, the average generation of the population grows linearly in time $G(t)/Z(t) \sim gt$ for some $g > 0$. In the following section we give a deterministic result to provide non-probabilistic intuition for why this is so before considering the stochastic system.

The clinching result quantitatively relates the phenomena of stochastic delabeling to generational expansion. So long as label-positive cells remain

$$\log \left(\frac{Z^+(t)}{Z(t)} \right) \stackrel{t \text{ large}}{\sim} \log(\exp((\alpha^+ - \alpha)t)) = (\alpha^+ - \alpha)t \stackrel{p \text{ small}}{\sim} -pgt,$$

so that for p small

$$\frac{G(t)}{Z(t)} \sim -\frac{1}{p} \log \left(\frac{Z^+(t)}{Z(t)} \right).$$

This identification holds for any age dependent branching process and does not depend upon the details of life-time distributions or the possibility of cell death, so long as populations do not go extinct.

The estimators are related through stochastic quantities and are subject to sample-path fluctuations, particularly at early time-points. Establishing that estimates, as a function of time on individual

sample paths, converge to the true average generation underlies the development of the two time-point estimator in equation (2). That methodology circumvents this issue of small number variability by eliminating the early fluctuations on a path-by-path basis. As a supporting result, we also prove that the path-to-path variability of estimates decreases inversely proportionally to the number of progenitors, supporting the precision of estimates for experimental systems that are initiated with multiple cells, which is typically the case.

4 Formal Results

4.1 In-expectation derivation

We begin by deriving a version of eq. (1) based on averages over realisations of the delabeling process. This derivation has the advantage that it requires no assumptions regarding the family tree and so holds in complete generality, but it is not informative with regards individual realisations. Sample-path, time-dependent properties of the estimators arise as a consequence of involved theorems in the context of the most well established generative model of family trees, age dependent branching processes, which follow this derivation.

At some time t , consider a collection of $Z(t)$ cells, whose familial relationship need not be known. The generation of a cell is defined to be the number of ancestors it possesses, with initial cells being defined to be in generation 0. Denote each of the generations of the $Z(t)$ cells by $g_1(t), \dots, g_{Z(t)}(t)$. of the generations of all living cells being denoted by

$$G(t) = \sum_{i=1}^{Z(t)} g_i(t),$$

knowing p we wish to estimate the average generation of presently living cells, i.e. $G(t)/Z(t)$, by observation of the proportion $Z^+(t)/Z(t)$.

If initial cells are label positive and with each division the label is lost independently with probability p , the probability cell i is still label positive in generation $g_i(t)$ is $(1-p)^{g_i(t)}$. With $Z^+(t)$ denoting the number of label positive cells, by linearity of expectation the average proportion of label-positive cells in the population is

$$\frac{E(Z^+(t))}{Z(t)} = \frac{1}{Z(t)} \sum_{i=1}^{Z(t)} (1-p)^{g_i(t)}.$$

Identifying $\theta = \log(1-p)$, this can be re-written in a form that identifies it with a moment generating function, e.g. [14],

$$E(e^{\theta\Gamma}) = \frac{1}{Z(t)} \sum_{i=1}^{Z(t)} \exp(\theta g_i(t)),$$

where Γ is uniformly selected in $\{g_1(t), \dots, g_{Z(t)}(t)\}$. As both the moment generating function and the cumulant generating function, $\log E(e^{\theta\Gamma})$, are real analytic, we can take a Taylor expansion of the latter around the origin, giving

$$\log(E(e^{\theta\Gamma})) = 0 + \theta E(\Gamma) + O(\theta^2),$$

so that

$$\lim_{\theta \rightarrow 0} \frac{1}{\theta} \log (E(e^{\theta \Gamma})) = E(\Gamma).$$

Taking $\theta \rightarrow 0$ is equivalent to taking $p \rightarrow 0$. Thus noting that $\lim_{p \rightarrow 0} p / \log(1 - p) = -1$, we obtain

$$\lim_{p \rightarrow 0} \frac{-1}{p} \log \left(\frac{E(Z^+(t))}{Z(t)} \right) = \frac{G(t)}{Z(t)},$$

which is formula (1), albeit with an expectation over stochastic delabelings. While this result is not as strong as others we shall prove, it illustrates both how the unusual formulation arises and that, averaged over delabeling processes, the relationship holds for arbitrary family tree structure.

4.2 Sample path properties

To determine sample path properties of the generation counting estimator, we must establish two quantitative relationships in a general age-dependent branching process: (1) relating the growth rates of labeled and unlabeled populations when the probability of delabeling per cell division is small; and (2) for the relationship between the number of cells alive and the sum of the generations of all living cells.

For the quantitative relationship between the growth-rates of the labeled and unlabeled populations when the delabeling probability per cell division is small and label-state does not impact on population dynamics, we leverage well-know single type results [27, 3]. For the relationship between the number of cells alive and the sum of the generations of all living cells, there are some results indirectly available from [55], but to identify more properties of our estimator we find it beneficial to provide an analysis of the joint probability generating function of number of cells alive and their total generation number.

Our initial mathematical study treats systems that start with a single initiating progenitor. From these results, systems that start with several statistically equivalent progenitors with indistinguishable progeny can be deduced. In addition, we provide results on the behavior of the estimator for a system with numerous progenitors, establishing that that variances behave inversely proportionally to the number of progenitors.

4.3 Smoothness of the Malthus parameter

We begin by considering a standard age dependent branching process, e.g. [22, 29], with the usual assumptions on the distribution of a lifetime, a non-negative random variable τ , and the number of offspring, N a non-negative integer valued random variable, at the end of a lifetime. In the circumstances of interest to us, proliferating cell populations, N will take values in $\{0, 2\}$ indicating that cells die or divide into two at the end of their lives, but we will prove the results in greater generality.

Assumption 1. *The lifetime distribution, $P(\tau \leq t)$ for $t \in [0, \infty)$, is non-lattice and satisfies $P(\tau \leq 0^+) = 0$. The probability generating function of the number of offspring, $\rho_N(s) = E(s^N)$ for $s \in \mathbb{R}$, is finite in a neighborhood of 1. We denote its expected value by $h = E(N) = \frac{d}{ds} \rho_N(s)|_{s=1}$.*

A key quantity in the study of age-dependent branching processes is the Malthus parameter, $\alpha(h)$, which is defined to be the solution of the following equation, should the solution exist,

$$hE(e^{-\alpha(h)\tau}) = 1. \quad (3)$$

If $\alpha(h)$ exists, it is then the, possibly negative, asymptotic exponential growth rate of the expected population size. The dependence of the Malthus parameter, $\alpha(h)$, on the expected number of offspring of a cell, h , is not usually made explicit, but will prove essential for us as we shall be interested in relating the growth rate of the label-positive population and of the total population, which will differ. For that purpose, we have the following result on the range of mean offspring, h , for which the Malthus parameter exists and its smoothness as a function of h . We expect that this Proposition is known, but cannot find a reference in the literature and so present a proof here.

Proposition 1. *Define*

$$\beta_{max} := \sup \{ \beta : E(e^{\beta\tau}) < \infty \} \text{ and } h_{min} := \inf \{ h : hE(e^{\beta_{max}\tau}) \geq 1 \},$$

where $h_{min} \leq 1$, then there exists a real analytic function $\alpha : (h_{min}, \infty) \mapsto \mathbb{R}$, the Malthus parameter, such that

$$hE(e^{-\alpha(h)\tau}) = 1 \text{ for } h \in (h_{min}, \infty).$$

In particular, for $h > h_{min}$, the first two derivatives of $\alpha(h)$ as a function of the average number of offspring h are

$$\alpha'(h) := \frac{d}{dh}\alpha(h) = \frac{1}{h^2 E(\tau e^{-\alpha(h)\tau})} \quad (4)$$

and

$$\alpha''(h) := \frac{d^2}{dh^2}\alpha(h) = \frac{1}{h^3 E(\tau e^{-\alpha(h)\tau})} \left(\frac{E(\tau^2 e^{-\alpha(h)\tau})}{h E(\tau e^{-\alpha(h)\tau})^2} - 2 \right). \quad (5)$$

Proof. Consider the function $g : (0, \infty) \times \mathbb{R} \mapsto [0, \infty]$ defined by

$$g(h, \beta) = hE(e^{-\beta\tau}) - 1. \quad (6)$$

We wish to identify the range of h such that $\alpha(h)$ exists satisfying $g(h, \alpha(h)) = 0$, and to determine its smoothness properties as a function of h . When $\beta = 0$, $E(e^{-\beta\tau}) = 1$ and so $h_{min} \leq 1$. As $E(e^{-\beta\tau})$ is the moment generating function of a non-negative random variable, τ , evaluated at $-\beta$, it is a real analytic function on the interior of the domain on which it is finite, i.e. for $\beta \in (-\beta_{max}, \infty)$. Therefore as $g(h, \beta)$ defined in eq. (6) is a product of real analytic functions, it is also real analytic on $(0, \infty) \times (-\beta_{max}, \infty)$. As $g(h, \beta)$ is a monotonic decreasing function of β , for any $h \in (h_{min}, \infty)$ there exists a unique β such that $g(h, \beta) = 0$. Thus we can apply the real analytic version of the Implicit Function Theorem, e.g. Theorem 1.8.3 [33]. This establishes that $\alpha(h)$ satisfying eq. (3) exists for $h \in (h_{min}, \infty)$, that α is real analytic for $h > h_{min}$, and that its first derivative satisfies

$$\alpha'(h) = - \frac{\partial}{\partial h} g(h, \beta)|_{(h, \alpha(h))} \Big/ \frac{\partial}{\partial \beta} g(h, \beta)|_{(h, \alpha(h))},$$

which gives eq. (4). To obtain eq. (5), one differentiates eq. (4). □

The real analyticity of $\alpha(h)$ allows us to characterize the difference in growth rates of two populations in terms of the Taylor expansion of $\alpha(h)$. This will be useful as if there is small probability of label-loss, then the label-positive and total populations have similar, but non-identical, average offspring number. We will relate the difference in their growth rates to the dynamics of the average generation of the population.

4.4 One way labeling populations

We consider a two-type reducible age-dependent branching process previously studied, for example, in [26]. That is, we consider a cell system that starts with a single progenitor that is positive for a label so that $Z^+(0) = 1$ and $Z^-(0) = 0$, and define the total population at time t to be $Z(t) = Z^+(t) + Z^-(t)$. Each cell is assumed to have an independent and identically distributed lifetime at the end of which they independently give rise to a random number of offspring. Positive label cells can become negative label cells, but the reverse does not happen. We are interested in populations where the label does not indicate a phenotypic change so that lifetime distributions do not depend on the label.

Depending upon the experimental system and marker employed, the process of delabeling can occur in different ways and so one may have distinct models. Thus we make a general assumption that encompasses several of these. Notationally, let the random variable $N^+(p)$ define the number of label-positive offspring of a label-positive cell, where $p \in (0, 1)$ captures the probability of delabeling. We will make a technical assumption that ensures that the distribution of the number of label-positive offspring of a label-positive cell is less than its total (i.e. label positive and negative) offspring and that as p drops to 0 we assume that we recover the random variable describing the total (i.e. label independent) offspring of a cell, denoted $N := N^+(0)$.

Assumption 2. *Lifetimes are independent and identically distributed, and independent of independent and identically distributed type-dependent offspring numbers. The lifetime distribution for cells, $P(\tau \leq t)$ for $t \in [0, \infty)$, is non-lattice and satisfies $P(\tau \leq 0^+) = 0$. If $p > 0$, the number of label-positive offspring of a label-positive cell is less than its total number of offspring: $N^+(p)$ is strictly stochastically dominated by $N = N^+(0)$, i.e. $P(N^+(p) \leq n) \geq P(N \leq n)$ for all $n \in \{0, 1, \dots\}$ and $P(N^+(p) \leq n) > P(N \leq n)$ for some n . Thus, defining $E(N^+(p)) = h_+(p)$, $h_+(p) < E(N) = h$ for all $p > 0$. We assume that $\rho_N(s) = E(s^N)$ for $s \in \mathbb{R}$, is finite in a neighborhood of 1, that $\lim_{p \downarrow 0} h_+(p) = h$, and that $h_+(p)$ is real analytic in p .*

Example 1: delabeling occurs immediately prior to a cell's division, independently with probability p . In this case the offspring of a label-positive cell's are either all labeled or all delabeled. Thus with N denoting the label-independent offspring random variable,

$$E\left(s^{N^+(p)}\right) = p + (1-p)E\left(s^N\right) = p + (1-p)\rho_N(s)$$

and, in particular, $h_+(p) = (1-p)h$.

Example 2: delabeling of the offspring of a label-positive cell occurs independently with probability p at birth. In this case

$$E\left(s^{N^+(p)}\right) = \sum_{n \geq 0} s^n \sum_{m \geq n} P(N = m) \binom{m}{n} (1-p)^n p^{m-n},$$

so that again $h_+(p) = (1-p)h$, but higher order moments are smaller than those in Example 1.

Example 3: the offspring of a label-positive cell experience asymmetric label-loss. There are genetic constructs where, on division, labels are lost asymmetrically [73]. That is, if a label-positive cell divides in two and one of its two offspring loses its label, then the other does not. As a result, if p is the probability of delabeling and q is the probability that a division rather than death occurs, then

$$E\left(s^{N^+(p)}\right) = q\left(sp + s^2(1-p)\right),$$

$E(N) = h = 2q$ and the mean number of label positive offspring is $E(N^+(p)) = h_+(p) = (1-p/2)h$.

In all three of these examples $h_+(p)$ is a linear function of p , so that Assumption 2 holds. Based on results in [27, 3] in conjunction with Proposition 1, the following theorem can be deduced.

Theorem 1. *If $h_+(p) > 1$, under Assumption 2, if $\lim_{t \rightarrow \infty} Z^+(t) > 0$, then almost surely*

$$\begin{aligned} \lim_{t \rightarrow \infty} \frac{1}{t} \log \left(\frac{Z^+(t)}{Z(t)} \right) &= \alpha(h_+(p)) - \alpha(h) \\ &= ph'_+(0)\alpha'(h) + \frac{1}{2}p^2(h'_+(0)^2\alpha''(h) + \alpha'(h)h''_+(0)) + O(p^3), \end{aligned} \quad (7)$$

where

$$h'_+(0) = \frac{d}{dp}h_+(p)|_{p=0} \text{ and } h''_+(0) = \frac{d^2}{dp^2}h_+(p)|_{p=0},$$

and, in particular, if $\lim_{t \rightarrow \infty} Z^+(t) > 0$, then almost surely

$$\lim_{p \rightarrow 0} \lim_{t \rightarrow \infty} \frac{1}{pt} \log \left(\frac{Z^+(t)}{Z(t)} \right) = h'_+(0)\alpha'(h). \quad (8)$$

Proof. The asymptotic behavior of $Z^+(t)$ and $Z(t)$ follow directly from [27, 3]. By Proposition 1, $\alpha(h)$ is real analytic for $h > h_{\min}$ and $1 \geq h_{\min}$, and, by Assumption 2, $h_+(p)$ is real analytic with $\lim_{p \downarrow 0} h_+(p) = h$. Thus $\alpha(h_+(p))$ is real analytic and we can take a Taylor expansion of $\alpha(h_+(p))$ in p around 0 and so eq. (7) holds. The relationship in (8) follows from eq. (7) taking the limit as p tends to 0. \square

For comparison with these two-population results, we need to establish properties of the total generation, the sum of the generations of living cells, for a single-type population.

4.5 Total generation of a branching process

In order to precisely define the total generation of a branching process, some unwieldy definitions are necessary. These shall be largely side-stepped in the analysis, but are included to precisely define the objects of interest to us. We use a modification of ideas in [22] to do so and consider a single-type construction as that is sufficient for our needs.

The generation of an object is defined to be the number of ancestors it possesses. As such, it is natural to begin with a single object at time 0 defined to be in generation 0. Let $\tau_j^{(i)}$ denote the length of the life of the j -th object in the i -th generation and let $N_j^{(i)}$ denote the number of offspring of the j -th

object in the i -th generation. Starting with a single object, the total number of objects that will, at any stage, exist in the n -th generation is governed by a Galton-Watson recursion:

$$K_0 = 1 \text{ and } K_{n+1} = \sum_{k=1}^{K_n} N_k^{(n)} \text{ for } n \geq 1,$$

where the empty sum is defined to be 0. That is, the number of objects that will ever be in generation 1 is the offspring number of the first object, $K_1 = N_1^{(0)}$. The number of offspring that will ever exist in generation 2 is the sum of the number offspring of those members of generation 1, and so forth, leading to the above recursion for K_n .

Each object in generation n is defined by a life-history, $\langle i_0, \dots, i_n \rangle$, where this object is the i_n -th child of the i_{n-1} -child of the i_{n-2} -th child and so forth back to $i_0 = 0$. The indices run over objects that exist, so that $i_n \in \{1, \dots, K_n\}$. The birth time of the object $\langle i_0, \dots, i_n \rangle$ is the sum of lifetime of its ancestors,

$$T_{\langle i_0, \dots, i_n \rangle} = \sum_{k=0}^{n-1} \tau_{i_k}^{(k)}.$$

The time the object ceases to be is $T_{\langle i_0, \dots, i_n \rangle} + \tau_{i_n}^{(n)}$. In terms of these definitions, the total number of objects present at time t can be identified as all objects of any generation that are alive at time t ,

$$Z(t) = \sum_{n=0}^{\infty} \sum_{\langle i_0, \dots, i_n \rangle} \chi \left(T_{\langle i_0, \dots, i_n \rangle} \leq t < T_{\langle i_0, \dots, i_n \rangle} + \tau_{i_n}^{(n)} \right) \quad (9)$$

where χ is the indicator function. That is, the population alive at time t is all those objects whose birth time is before or equal to t and whose death time is after t .

The generation of an object $\langle i_0, \dots, i_n \rangle$ is n and thus the sum of the generations of all objects existing at time t is

$$G(t) = \sum_{n=0}^{\infty} n \sum_{\langle i_0, \dots, i_n \rangle} \chi \left(T_{\langle i_0, \dots, i_n \rangle} \leq t < T_{\langle i_0, \dots, i_n \rangle} + \tau_{i_n}^{(n)} \right). \quad (10)$$

That is, for each object alive at time t in generation n , the total generation at that time is incremented by n .

Before considering the probabilistic system, we begin with a fundamental, non-probabilistic lemma that will give an indication as to why one expects that the total generation of all living cells G to grow in a similar fashion to $Z \log Z$, where Z is the number of presently living cells, assuming that cells can either die or divide into two at the end of their lives.

Lemma 1. *For a binary family tree beginning with a single progenitor in generation 0, if there are $Z > 0$ cells alive then the average generation per cell satisfies $G/Z \geq \log_2 Z$.*

Proof. Consider a family tree with $Z = 2^n + m$ cells alive (i.e. Z leaves), where $n \in \{0, 1, \dots\}$ and $m \in \{0, 1, \dots, 2^{n+1} - 2^n\}$. The minimal G given Z is attained is when $2^n - m$ cells are in generation

n and $2m$ cells are in generation $n + 1$, which can be formally established using the equations given above. Thus

$$Z \log_2 Z = (2^n + m) \log_2(2^n + m) \text{ and } G = (2^n - m)n + 2m(n + 1).$$

If $m = 0$ or $m = 2^n$, these are equal and so the difference between the two is zero at each 2^n and one needs to be delicate with one's estimates. A rearrangement of terms gives $Z \log_2 Z \leq G$ if and only if

$$(2^n + m) \log_2(1 + m/2^n) \leq 2m.$$

A sufficient condition for this to be true is to relax the problem, letting $m = x2^n$ with $x \in [0, 1]$, and establish that

$$(1 + x) \log_2(1 + x) \leq 2x \text{ for all } x \in [0, 1],$$

which is readily achieved by calculus. □

In a system with death, in general there is no equivalent upper bound to Lemma 1 as it's possible that there is only one cell alive, $Z = 1$, and the generation of that cell, and hence G , can be arbitrarily large. For branching processes, however, under general conditions the population either dies out or ultimately grows in a somewhat regular fashion, [22], and so Lemma 1 anticipates that, in a suitable sense, $G(t)/(tZ(t))$ becomes constant if the population survives. Indeed, amongst other results, this is something we shall establish.

It is not possible to study the total generation of living cells, $G(t)$, separately from the total population, $Z(t)$, as they are strongly coupled and their dynamics are intertwined. This relationship appears as a cross term in eq. (12) when we consider the evolution of the joint probability generating function of the two, giving rise to an integral equation of unusual form. Despite this form, it is, in general, susceptible to analysis.

Assumption 3. *Lifetimes are independent and identically distributed and independent of independent and identically distributed offspring numbers. The lifetime distribution, $P(\tau \leq t)$ for $t \in [0, \infty)$, is non-lattice and satisfies $P(\tau \leq 0^+) = 0$. The probability generating function of the number of offspring, $\rho_N(s) = E(s^N)$ for $s \in \mathbb{R}$, is finite in a neighborhood of 1. We denote its first and second derivative at one by*

$$h = E(N) = \frac{d}{ds} \rho_N(s)|_{s=1} \text{ and } v = E(N^2) - h = \frac{d^2}{ds^2} \rho_N(s)|_{s=1}. \quad (11)$$

Theorem 2. *Under Assumption 3, starting with $(Z(0), G(0)) = (1, 0)$, the joint probability generating function of $\{(G(t), Z(t))\}$,*

$$\rho_{G,Z}(s_g, s_z, t) := E \left(s_g^{G(t)} s_z^{Z(t)} \right),$$

satisfies the integral equation

$$\rho_{G,Z}(s_g, s_z, t) = P(\tau > t) s_z + \int_0^t dP(\tau \leq u) \rho_N(\rho_{G,Z}(s_g, s_g s_z, t - u)). \quad (12)$$

For $h > h_{min}$, define

$$c(h) = \frac{\alpha'(h)(h - 1)}{\alpha(h)}, \quad (13)$$

where $\alpha(h)$ and $\alpha'(h)$ are defined in the statement of Proposition 1. For $h > h_{\min}$,

$$\lim_{t \rightarrow \infty} \frac{E(G(t))}{te^{\alpha(h)t}} = c(h)h\alpha'(h), \quad (14)$$

and

$$\lim_{t \rightarrow \infty} \frac{E(G(t))}{tE(Z(t))} = h\alpha'(h). \quad (15)$$

If $h > 1$, with v defined in eq. (11), defining

$$\kappa = \frac{vE(e^{-2\alpha\tau})}{1 - hE(e^{-2\alpha\tau})}, \quad (16)$$

in addition we have that

$$\lim_{t \rightarrow \infty} \frac{E(G(t)Z(t))}{tE(Z(t))^2} = h\alpha'(h)\kappa \text{ and } \lim_{t \rightarrow \infty} \frac{E(G(t)^2)}{t^2E(Z(t))^2} = (h\alpha'(h))^2 \kappa.$$

Proof. We first establish that eq. (12) holds. Begin with a family tree starting with a single cell at time 0, $Z(0) = 1$, defined to be in generation 0, so that $G(0) = 0$. Consider the impact of altering this initial condition so that the founding cell is in generation 1 at $t = 0$, $G(0) = 1$. We will write $G_1(t)$ for the process counting the total generation of living cells starting with $G(0) = 1$, so that, in particular, $G_1(0) = 1$, and retain $G(t)$ for total generation given $G(0) = 0$. The key observation, which can be established using equations eq. (10) and eq. (9), is that

$$G_1(t) = \sum_{n=1}^{\infty} (n+1) \sum_{\langle i_1, \dots, i_n \rangle} \chi \left(T_{\langle i_1, \dots, i_n \rangle} \leq t < T_{\langle i_1, \dots, i_n \rangle} + \tau_{i_n}^{(n)} \right) = G(t) + Z(t).$$

This can be understood by noting that, leaving all other aspects of the family tree unchanged, the move from $G(0) = 0$ to $G(0) = 1$ causes the generation of every living cell to increase by 1.

Thus, taking expectations over the lifetime of the initial cell and using the independence and identical distribution of the sub-trees generated by the first birth, but noting they start with cells that are in generation 1, we obtain

$$\begin{aligned} \rho_{G,Z}(s_g, s_z, t) &= P(\tau > t)s_z + \int_0^t dP(\tau \leq u)\rho_N \left(E \left(s_g^{G_1(t-u)} s_z^{Z(t-u)} \right) \right) \\ &= P(\tau > t)s_z + \int_0^t dP(\tau \leq u)\rho_N \left(E \left(s_g^{G(t-u)+Z(t-u)} s_z^{Z(t-u)} \right) \right) \\ &= P(\tau > t)s_z + \int_0^t dP(\tau \leq u)\rho_N \left(E \left(s_g^{G(t-u)} (s_g s_z)^{Z(t-u)} \right) \right) \\ &= P(\tau > t)s_z + \int_0^t dP(\tau \leq u)\rho_N (\rho_{G,Z}(s_g, s_g s_z, t-u)), \end{aligned}$$

giving eq. (12). The uniqueness of $\rho_{G,Z}(s_g, s_z, t)$ for $s_g < 1$ and $s_z < 1$ follows from analogous arguments to those in [22], Chapter VI, utilizing the ideas in [35].

To establish eq. (14), note that using eq. (12)

$$\begin{aligned} E(G(t)) &= \frac{\partial \rho_{G,Z}(s_g, s_z, t)}{\partial s_g} \Big|_{s_g=s_z=1} = \int_0^t dP(\tau \leq u) h E(G(t-u)) + \int_0^t dP(\tau \leq u) h E(Z(t-u)) \\ &= \int_0^t dP(\tau \leq u) h E(G(t-u)) + E(Z(t)) - P(\tau > t), \end{aligned}$$

where we have used the equivalent, well known integral equation for $E(Z(t))$ to obtain the final equality. We wish to study the asymptotics of this equation, dividing it by $t \exp(\alpha(h)t)$ and taking limits as $t \rightarrow \infty$. To this end, we employ a result from renewal theory, [2] Theorem 6.2(a), using the fact that by construction $h \exp(-\alpha(h)t) dP(\tau \leq t)$ is a probability measure,

$$\lim_{t \rightarrow \infty} \frac{E(G(t))}{t e^{\alpha(h)t}} = \frac{1}{h E(\tau e^{-\alpha(h)\tau})} \left(\lim_{t \rightarrow \infty} e^{-\alpha(h)t} E(Z(t)) - \lim_{t \rightarrow \infty} e^{-\alpha(h)t} P(\tau > t) \right),$$

should the limits on the right hand side exist. The existence of the first limit follows from results in [22],

$$\lim_{t \rightarrow \infty} e^{-\alpha(h)t} E(Z(t)) = c(h). \quad (17)$$

Consider $e^{-\alpha(h)\tau} P(\tau > t)$. If $\alpha(h) > 0$, then the limit automatically exists and is 0. If $\alpha(h) < 0$, select $\beta > -\alpha(h) > 0$ such that $E(\exp(\beta\tau)) < \infty$. From Proposition 1, we are guaranteed the existence of such a β as $h > h_{\min}$. As $\beta > 0$, as in the Chernoff bound we have that

$$P(\tau > t) = E(1_{\{\tau > t\}}) \leq e^{-\beta t} E(e^{\beta\tau}) \text{ and hence } \limsup_{t \rightarrow \infty} e^{\beta t} P(\tau > t) \leq E(e^{\beta\tau}).$$

As $\beta > -\alpha(h)$, this ensures that

$$\lim_{t \rightarrow \infty} e^{-\alpha(h)t} P(\tau > t) = 0.$$

Hence, using eq. (4),

$$\lim_{t \rightarrow \infty} \frac{E(G(t))}{t e^{\alpha(h)t}} = c(h) h \alpha'(h),$$

as required. To obtain eq. (15), one uses eq. (17) in conjunction with eq. (14).

Consider now, with a little re-arranging of terms,

$$\begin{aligned} E(G(t)Z(t)) &= \frac{\partial^2}{\partial s_z \partial s_g} \rho_{G,Z}(s_g, s_z, t) \Big|_{s_g=s_z=1} \\ &= \int_0^t dP(\tau \leq u) h E(G(t-u)Z(t-u)) + \int_0^t dP(\tau \leq u) h E(Z(t-u)^2) \\ &\quad + \int_0^t dP(\tau \leq u) v E(Z(t-u))^2 + \int_0^t dP(\tau \leq u) v E(G(t-u)) E(Z(t-u)). \end{aligned} \quad (18)$$

We wish to establish that the limit

$$\lim_{t \rightarrow \infty} \frac{E(G(t)Z(t))}{t e^{2\alpha(h)t}}$$

exists and identify its limit. Using eq. (17) and

$$\lim_{t \rightarrow \infty} e^{-2\alpha(h)t} E((Z(t)^2)) = c(h)^2 \kappa,$$

which can be found in [22], it is clear that only the last term on the right hand side of (18) could be non-zero. As $e^{-2\alpha(h)t} dP(\tau \leq t)$ is a defective probability measure, that is $\int_0^\infty e^{-2\alpha(h)t} dP(\tau \leq t) < 1$, an application of the Renewal Theorem for Defective Measures [51] in conjunction with the Dominated Convergence Theorem leads us to

$$\begin{aligned} \lim_{t \rightarrow \infty} \frac{E(G(t)Z(t))}{te^{2\alpha(h)t}} &= \frac{v}{1 - hE(e^{-2\alpha(h)\tau})} \lim_{t \rightarrow \infty} \int_0^t e^{-2\alpha(h)u} dP(\tau \leq u) \frac{E(G(t-u))}{te^{\alpha(h)(t-u)}} \frac{E(Z(t-u))}{e^{\alpha(h)(t-u)}} \\ &= v \frac{E(e^{-2\alpha(h)\tau})}{1 - hE(e^{-2\alpha(h)\tau})} c(h)^2 h \alpha'(h) \\ &= c(h)^2 h \alpha'(h) \kappa. \end{aligned}$$

A similar argument reveals the other equality. □

From eq. (8) and eq. (15), in Theorems 1 and 2 respectively, we have our cornerstone result relating the average generation of the population to the proportion of positively labeled cells, justifying (1) and (2).

Proposition 2. *Under Assumptions 1 and 2, if $\lim_{t \rightarrow \infty} Z^+(t) > 0$, then*

$$\lim_{t \rightarrow \infty} \frac{E(G(t))}{tE(Z(t))} = h\alpha'(h) = \lim_{p \rightarrow 0} \lim_{t \rightarrow \infty} \frac{1}{pt} \log \left(\frac{Z^+(t)}{Z(t)} \right) \left(\frac{h}{h'_+(0)} \right)$$

almost surely.

Consider the delabeling possibilities described after Assumption 2. In Examples 1 and 2, where delabeling occurs with probability p at the end of a lifetime or independently with probability p for each offspring, $h/h'_+(0) = -1$ and we have that

$$\lim_{t \rightarrow \infty} \frac{E(G(t))}{tE(Z(t))} = - \lim_{p \rightarrow 0} \lim_{t \rightarrow \infty} \frac{1}{pt} \log \left(\frac{Z^+(t)}{Z(t)} \right),$$

almost surely, if $\lim_{t \rightarrow \infty} Z^+(t) > 0$. Whereas, as in Example 3, if delabeling occurs via an asymmetric division construct, $h/h'_+(0) = -2$ so that

$$\lim_{t \rightarrow \infty} \frac{E(G(t))}{tE(Z(t))} = -2 \lim_{p \rightarrow 0} \lim_{t \rightarrow \infty} \frac{1}{pt} \log \left(\frac{Z^+(t)}{Z(t)} \right).$$

almost surely if $\lim_{t \rightarrow \infty} Z^+(t) > 0$.

We have proved results for $E(G(t))/E(Z(t))$, experimentally we would wish to know $E(G(t)/Z(t))$, the average generation per progenitor. Thus we wish to establish that these results are a good approximation for the latter. To achieve this we use the standard approach, e.g. [62], of taking a Taylor expansion of the ratio around the ratio of the expectations, and quantifying how the expectation

of its leading order terms behave. Using the first and second order terms of the Taylor expansion, we have

$$E\left(\frac{G(t)}{Z(t)} \mid Z(t) > 0\right) \approx \frac{E(G(t))}{E(Z(t))} \left(1 + \frac{E(Z(t)^2)}{E(Z(t))^2}\right) - \frac{E(G(t)Z(t))}{E(Z(t))^2}.$$

Using the results in Theorem 2, if $h > h_{\min}$

$$\lim_{t \rightarrow \infty} \frac{1}{t} \left(\frac{E(G(t))}{E(Z(t))} \left(1 + \frac{E(Z(t)^2)}{E(Z(t))^2}\right) - \frac{E(G(t)Z(t))}{E(Z(t))^2} \right) = h\alpha'(h) = \lim_{t \rightarrow \infty} \frac{E(G(t))}{tE(Z(t))}.$$

Thus using the ratio of the expectations as an approximation to the expectation of the ratio is reasonable.

We can also use the Taylor approximation to determine the approximate behavior of the variance of $G(t)/Z(t)$. Namely, to first order

$$\begin{aligned} E\left(\left(\frac{G(t)}{Z(t)}\right)^2 \mid Z(t) > 0\right) - E\left(\frac{G(t)}{Z(t)} \mid Z(t) > 0\right)^2 \\ \approx \frac{E(G(t)^2)}{E(Z(t))^2} - \frac{2E(G(t)Z(t))E(G(t))}{E(Z(t))^3} + \frac{E(G(t))^2E(Z(t)^2)}{E(Z(t))^4}. \end{aligned}$$

Using the results in Theorem 2, if $h > 1$, this shows that the variance is becoming small,

$$\lim_{t \rightarrow \infty} \left(\frac{E(G(t)^2)}{t^2E(Z(t))^2} - \frac{2E(G(t)Z(t))}{tE(Z(t))^2} \frac{E(G(t))}{tE(Z(t))} + \left(\frac{E(G(t))}{tE(Z(t))}\right)^2 \frac{E(Z(t)^2)}{E(Z(t))^2} \right) = 0.$$

Thus we expect the average generation of a population of cells to be a stochastically well behaved process; a phenomenon we will observe in simulations described later.

4.6 Large numbers of progenitors

Cultures are typically started with more than a single progenitor and so one expects that the estimator's accuracy will improve by laws of large numbers. Here, by means that have nothing to do with branching processes, we establish that this is indeed the case and that, in particular, the ratios are both Asymptotically Normal, e.g. [56], and the variance decreases as one over the number of progenitors.

In order to state the result, recall that a sequence of random variables $\{X_n\}$ is said to be Asymptotically Normal, e.g. [56], with means $\{\mu_n\}$ and variances $\{\sigma_n^2\}$ if $\sigma_n > 0$ for all n sufficiently large and the sequence $\{(X_n - \mu_n)/\sigma_n\}$ converges in distribution to $N(0, 1)$, the Gaussian distribution with mean 0 and variance 1.

Theorem 3. *Let $\{(Z^+_i(t), Z_i(t))\}$ be a bivariate i.i.d sequence of possibly correlated random variables, representing the label-positive and total cell population at time t from progenitor i , and let (Z^+, Z) be an independent copy. If the probability generating function of (Z^+, Z) is finite in a neighbourhood of $(1, 1)$, then*

$$-\frac{1}{p} \log \left(\frac{\sum_{i=1}^n Z^+_i(t)}{\sum_{i=1}^n Z_i(t)} \right)$$

is Asymptotically Normal with

$$\mu_n = -\frac{1}{p} \log \frac{E(Z^+)}{E(Z)} \text{ and } \sigma_n^2 = \frac{1}{n} \frac{1}{p^2} \left(\frac{\text{Var}(Z^+)}{E(Z^+)^2} - 2 \frac{\text{Cov}(Z^+, Z)}{E(Z^+)E(Z)} + \frac{\text{Var}(Z)}{E(Z)^2} \right), \quad (19)$$

where $\text{Cov}(X, Y) = E((X - E(X))(Y - E(Y)))$ and $\text{Var}(X) = \text{Cov}(X, X)$.

Let $\{(G_i(t), Z_i(t))\}$ be a bivariate i.i.d sequence of possibly correlated random variables, representing the total generation and total cell population at time t from progenitor i , and let (G, Z) be an independent copy. If the probability generating function of (G, Z) is finite in a neighbourhood of $(1, 1)$, then $\sum_{i=1}^n G_i(t) / (\sum_{i=1}^n Z_i(t))$ is Asymptotically Normal with

$$\mu_n = \frac{E(G)}{E(Z)} \text{ and } \sigma_n^2 = \frac{1}{n} \left(\frac{\text{Var}(G)}{E(Z)^2} - 2 \frac{\text{Cov}(G, Z)E(G)}{E(Z)^3} + \frac{\text{Var}(Z)E(G)^2}{E(Z)^4} \right). \quad (20)$$

Proof. Both results start with an application of the Multi-variate Central Limit Theorem, e.g. [56], to the partial sums of $\{(Z^+_i(t), Z_i(t))\}$ and $\{(G_i(t), Z_i(t))\}$ to establish their Asymptotic Normality. Application of the Delta Method, the corollary on page 124 of [56], with the function $g(x, y) = x/y$ then establishes Asymptotic Normality of the ratios of the sums. An additional application of the Delta Method with the function $g(x) = -p^{-1} \log(x)$ establishes the Asymptotic Normality of the logarithm of the ratio of sums. \square

As a result of this theorem, we anticipate the variability in the average generation number, as well as the variability in estimator, to decrease significantly as the number of progenitors increases.

5 Validation Using Simulated Data

Here we use Monte Carlo simulations of age dependent branching processes [22, 29] to validate the method, investigating its appropriateness on individual stochastic sample paths for parameter values of the order one would anticipate experimentally.

Define $Z^+(t)$ to be the number of label-positive live cells at time t , $Z(t)$ to be the total number of living cells at time t , $G(t)$ to be the sum of the generations of all living cells at time t , so that $G(t)/Z(t)$ is the average generation of living cells at time t . In this section each cell's lifetime is drawn independently from the same distribution and, at the end of their life, each cell independently either dies or gives rise to two cells. We assume that label-positive cells delabel immediately prior to division with probability p .

One of the estimator's primary features is that it can be used in practice without knowledge of the lifetime distribution or death rates. Thus we performed stochastic simulations over a range of conditions, including lifetime distributions such as lag-exponential, lag-log-normal and lag-gamma, and parameter values such as $p \in (10^{-5}, 10^{-1})$, $t \in [0, 300]$ hours and the average number of offspring of a cell, $E(N) = h$, in $(0, 2)$. These values include those typically encountered in cell cycle experiments [60, 24, 64, 65, 70, 71] and demonstrated the merits of the method, even for t being relatively small, at a few days, and p of order 0.01 per cell per generation. To illustrate the insights gained from the simulation study, we report on a specific, representative example, where lifetime distribution is lognormal, which is found to be a good fit in [24]. Figures 3 and 4 are the equivalents of 1 and 2, but for delayed-gamma distributed cell lifetimes. The results for both of these settings, as well as others that we have explored, are qualitatively similar.

5.1 Simulation parameterization

For the lifetime distribution we assume a log-normal distribution with parameter values based on data from long-term video microscopy of murine B lymphocytes proliferating in response to CpG DNA [24], τ is log-normally distributed with mean 9.3 hours and standard deviation $\sigma = 2.54$ hours. We consider populations that are, on average, expanding.

For the probability of delabeling, we adopt estimates related to existing division-linked labeling systems, namely Cre-induced mitotic recombination [65, 36] and micro-satellite mutation induced label activation [59, 30]. The probability of Cre induced mitotic recombination has been estimated for a specific construct as 10^{-2} per cell per generation [65], while mutation rates in human micro-satellites were inferred to be in the $(10^{-4}, 10^{-3})$ range per locus per generation [64].

Cell populations are simulated for $T = 250$ hours. At the end of a cell's lifetime, it divides into two cells with probability 0.8 and dies with probability 0.2, giving an average number of offspring $h = 1.6$. This leads to an average expansion by a factor of approximately 10^6 at 250 hours and an average increase in the generation number of more than 25. Note that 25 generations is far beyond what current experimental method, such as continuous observation or division-diluting dyes, are able to measure.

The mathematical results hold for sample population ratios where label-positive cells persist. If at some time $t \in (0, T]$ $Z^+(t) = 0$, we do not report the path from t on as this represent samples for which the experimenter would have no estimate beyond that time.

5.2 Single progenitors: generation consistency, label ratio variability at early times

Systems that start with a single label-positive cell are subject to the greatest variability at early times and thus this situation is the one that poses the greatest difficulties for estimation. While most experimental systems will start with more than a single progenitor and we know from the mathematical results in Section 4.6 that they are better behaved, with variance in estimates decreasing inversely proportional to starting cell number, we begin by considering this most challenging circumstance.

Starting with a single label-positive progenitor at $Z^+(0) = 1$, panels (a) and (b) of Fig. 1 plot 15 realizations of both the average generation $G(t)/Z(t)$ (orange lines) and the estimate of it, $-1/p \log(Z^+(t)/Z(t))$ (blue lines). The average generation across realizations is consistent, even for early times, and grows linearly in time as Theorem 2 predicts.

In contrast, the per-realization estimates, the blue lines, which the sample path theory establishes will ultimately grow with the same slope as the average orange line, exhibit substantial variability at short time-scales. Two dynamical properties contribute to these fluctuations. At the beginning, there are no label-negative cells and so the logarithm of the ratio is 0. When the first label-negative cells appear, the ratio of label-positive to total cell population can dramatically change, especially if the population size is small. In effect, the theorem is not in force until both the label positive and label negative populations are large enough for average behavior to become dominant, which only happens after at least an order of $1/p$ division events have occurred. As one might expect, by decreasing p from 10^{-2} to 10^{-3} this effect is amplified, as can also be seen in Fig. 1 (a) and (b).

In this setting, the typical behavior is initially for underestimation as can be seen in the inter-quartile

range plot of panels (c) and (d) of Fig. 1 for 10^4 simulations. This can be understood as there is no estimate prior to at least one cell delabeling, which requires, on average, $1/p$ divisions to occur. As p is assumed small, typically one does not initially get an estimate and this delay explains the observed lag in the blue lines. On the other hand, in the unlikely event that an early cell delabels, then the approximation eq. (1) initially gives significant over-estimates. This bias, which we have observed consistently across other simulations, suggests that if starting with a single progenitor family, eq. (1) only becomes accurate at longer time-frames, i.e. after several generations have passed. Note that the mean value of the estimator at early times over multiple runs is effected by outliers, hence the mean lies outside the inter-quartile range.

5.3 Single progenitors: mitigating variability by use of two time-points

Results in Section 4 for the time-dependent sample paths of estimates suggest that one way to mitigate this initial variability in the single time-point estimate $-1/p \log(Z^+(t)/Z(t))$ is to make two measurements at distinct times, $t_1 < t_2$ and use their difference to estimate $G(t)/Z(t)$ via the approximation eq. (2) in Section 1:

$$\frac{G(t)}{Z(t)} \approx \left(\frac{t}{t_2 - t_1} \right) \left(-\frac{1}{p} \log \left(\frac{Z^+(t_2)Z(t_1)}{Z^+(t_1)Z(t_2)} \right) \right).$$

The effect of this difference measurement is the removal of the initial fluctuations on a path-by-path basis. This is illustrated in Fig. 1, panels (e) and (f). Using Monte Carlo methods and a standard kernel estimation method, the plots compare three values: the actual average generation $G(t_2)/Z(t_2)$ at $t_2 = 250$ hours (orange); the single time-point estimates $-1/p \log(Z^+(t_2)/Z(t_2))$ (blue); and, with $t_2 = 250$ and an extra measurement at $t_1 = 200$ hours, the two time point estimates in eq. (2) with $t = t_2 = 250$ hours. The two-point estimate is not only more symmetrically distributed around the true value, but its variability is significantly less than the single time-point estimates.

5.4 Multiple progenitors: improved consistency

While the method works well for single progenitors, experiments are typically seeded with multiple progenitors. Theorem 3 establishes that the variability decreases inverse linearly with the number of progenitors, $Z(0)$, and so one expects that starting with even a small number of cells will eradicate the early time variability and here we demonstrate that this is, indeed, the case. For $Z^+(0) = 100$, Fig. 2 panels (a) and (b) correspond with those of Fig. 1. The orange lines, showing the per-realization of the average generation, remain largely unchanged, but the accuracy of the single time point estimates (blue) are greatly improved.

This comes about as even if an individual progenitor's family generates label-negative cells relatively late this is balanced by another progenitor's family where delabeling happened relatively early. Thus both $Z^+(t)$ and $Z(t)$ rapidly become sufficiently substantial for the limit theorem to be in force and for the estimator to be precise.

Fig. 2 panels (c) and (d) show Monte Carlo created Box plots of the per-sample average generation, the single time-point estimate and the two time-point estimate for a range of initial progenitor numbers. Sample-to-sample variation is greatly reduced even with as few as 10 progenitors. Thus in standard experimental systems, which are often seeded with hundreds or thousands of cells, the estimator is expected to be precise.

6 Validation Using Published Data

The simulations of the previous section show that the estimator works well for parameterizations akin to those found in experimental systems and provide insight into the impact of a number of factors, such as the delabeling probability and the number of progenitors, on the quality of the estimates. Here we use a range of published data to further investigate the estimator’s applicability.

6.1 Early development of *C. elegans*

The first application takes lineage trees of the early development of *C. elegans* determined by time-lapse microscopy and reported on in [52]. As the entire family tree is known, we have direct access to measurements of average generation as a function of time. Simulating a stochastic delabeling process on this tree, as would be experimentally possible via a division linked mosaic construct similar to the one introduced in [31] or the one we propose in Section 7, we can directly investigate the estimator’s accuracy.

Fig. 5 (a) shows the embryonic lineage tree of the nematode *Caenorhabditis elegans* as constructed from data published by Richards et al. [52]. In their study, a reference lineage tree was constructed based on output from automated tracking of nuclei in 18 embryos, recorded over approximately six hours at 1.5 minute intervals by three-dimensional resonance-scanning confocal microscopy. Each node in the figure represents a cell division and the tree contains information about all parent-daughter relationships and gives the timing of more than 10^3 division events during an embryo’s development. This leads to a population size of approximately 600 cells, Fig. 5 (b). From the timing of the division events, lifetimes are readily computed, shown in Fig. 5 (c).

For this tree, lifetime durations correlate positively with both generation and with the time of birth relative to fertilization, Fig. 5 (d), illustrating a lack of homogeneity. Regarding independence, there are correlations throughout the tree. Fig. 5 (e) demonstrates, for example, that lifetimes of siblings are positively correlated. These features are not in line with the assumptions under which some of the the sample path properties of the estimator were established, but are consistent with the derivation via properties of the cumulant generating function in Section 4.

To test the accuracy of the estimator, we stochastically decorated the tree. Beginning with a single label-positive progenitor, daughters are delabeled with probability p . Should they remain label-positive, their daughters are delabeled independently with probability p and so on for the whole tree. Fig. 5 (a) illustrates one such random decoration, with blue indicating label positive and white label negative.

For 10^4 independent Monte Carlo realizations of this delabeling process, Fig. 5 (f) shows the average (blue) and the inter-quartile range of the estimates (blue), using (1), at each time point during the first six hours of the development as well as the true average generation number of the embryo in orange, proving to be accurate.

As explained in Section 2, if not all cells are initially label-positive one can estimate average generation from proportion measurements at two distinct times. To mimic this, we considered the development of the labeled trees after $t_1 = 150$ minutes. At $t_1 = 150$ minutes one measurement is taken, giving the proportion of label-positive cells and the approximation eq. (2) to determine the average generation growth since t_1 to the time of a later measurement to determine the average generation since t_1 . The results are plotted in Fig. 5 (g), which show accuracy.

6.2 Micro-satellite mutation reporter systems

Existing micro-satellite reporter systems implement division-linked labeling and are suitable for both *in vitro* and *in vivo* applications [59, 16, 32, 30, 31]. Micro-satellites are short repeating motifs found in DNA that, with small probability per cell division, are subject to insertion or deletion of copies of the motif. Mutation reporter systems possess an initially out of frame gene for a fluorescent protein. Micro-satellite mutation on division results in the gene becoming in frame, with the cell becoming fluorescent. This fluorescent state is inherited by offspring and is either irreversible, as in [31], or has a reportedly negligible likelihood of reversion [16, 32]. Thus with micro-satellite mutation acting as a driver of rare division linked change, cell fluorescence serves as a label for average generation estimation.

The two data sets we analyze are from studies published by Gasche et al. [16] on human colorectal cancer cells (HCT116) and Kozar et al. [32] on mouse embryonic fibroblast (MEF). The probability that a cell becomes fluorescent as a result of a micro-satellite mutation is estimated as 6.1×10^{-4} and 1.1×10^{-4} in each study, respectively. For generation estimation, these values serve as p , the probability of delabeling per cell division.

The data sets consist of measurements of proportions of labeled cells over several days from *in vitro* proliferating cell lines that carry transgenic micro-satellite mutation reporter cassettes, allowing us to estimate the average generation of the cell population. In addition to the proportions, [32] also provides the growth curve, which is exponential from day one to day four before slowing down, probably as a consequence of cell confluence [32], while [16] reports an exponential growth for the whole time-course of their experiment.

Applying the estimator $-1/p \log(Z^+(t)/Z(t))$ with the proportions, $Z^+(t)/Z(t)$, recapitulated in Fig. 6 (a-b), and label loss probabilities provided in the studies, we can estimate the average generation $G(t)/Z(t)$ as a function of time, Fig. 6 (c). For both data sets, the estimated average generation increases linearly over time at a rate of approximately one per day.

Direct validation of the method with this data would require knowledge of the average generation, which is not reported in the above studies. The growth curve Fig. 6 (d), however, allows an alternate method to estimate this quantity for comparison. We directly estimate the average from this curve by assuming for exponentially distributed life-times and the absence of cell death as in this special case one can show that $E(G(t))/E(Z(t)) = 2\mu t$, where μ is the Malthus parameter [22, 29]. Estimating μ from the growth curve from day one up to day four, using linear regression on $\log(Z(t))$, predicts that the increase of average generation relative to the first time point as $1.06 t$. This prediction matches closely the estimated average generation, Fig. 6 (c). Taken together, the analysis of these data shows that inferring the average generation from the proportion of labeled cells carrying micro-satellite mutation reporter cassettes is an experimentally feasible approach.

7 Experiment Design

As an illustrative example of an ideal experiment including estimation of the probability of label-loss p , we describe one possible implementation of a division-linked one-way labeling system via a genetic construct, Fig. 7 (a), that combines existing experimental techniques: expression of a fluorescent protein such as Blue Fluorescent Protein (BFP); the use of a cell-cycle specific promoter to create division-linked changes [54, 4]; and site-specific recombination [44].

The construct is composed of two elements. First CRE recombinase expression is placed under the control of a cell-cycle specific promoter [54, 4]. The cell-cycle promoter is employed to ensure a division linked expression of CRE recombinase. Then, two LoxP sites are placed at each end of the BFP gene. As cells enter cell cycle CRE recombinase is expressed, site-specific recombination will occur probabilistically between the two LoxP recombination sites [44] and the BFP gene is excised.

For average generation inference, the desirable likelihood of recombination should be small, which can be achieved with a low efficiency CRE recombinase. Thus BFP+ cells are regarded as label positive and BFP- cells are label negative. This design is similar in spirit to an existing one used to create mosaics in Zebrafish [31], which employs micro-satellites as a division linked probabilistic driver and a kalooop in lieu of site-specific recombination.

The proportion of label-positive cells in a cell system incorporating this construct can be readily determined via fluorescence-activated cell sorting (FACS). The essential remaining ingredient for average generation inference is the determination of the probability of label-loss. This can be achieved by a *in vitro* FACS experiment, as illustrated by the *in silico* simulated experiment in Fig. 7 (b)-(c). A collection of cells that incorporate the construct are stained with a division diluting dye, such as CFSE [49], with noise added for illustrative purposes. After division, cells are gated based on their generation, and the proportion of label-positive cells per-generation determined by their fluorescence. With $\text{BFP}^+(n)$ being the measured proportion of label-positive cells in generation n , in the presence of a large number of initial progenitors the probability label-loss, p , irrespective of whether deaths occur, is $1 - \text{BFP}^+(n+1)/\text{BFP}^+(n)$, which should be the same for every n . In particular, if all initial cells are BFP+, then $\text{BFP}^+(0) = 1$ and $p = 1 - \text{BFP}^+(1) = \text{BFP}^-(1)$, the proportion of BFP negative cells in generation 1. Thus the probability of label-loss can be readily determined experimentally. For this simulation, an estimated value of p is determined using this measurement for $n = 0$, $p = \text{BFP}^-(1)$.

The accuracy of the method can then be checked during or after the experiment by comparing the average generation as determined by the division diluting dye with the value estimated via equation (1) with the measured p , Fig. 7 (d). Once p is known, similar cell stain experiments with distinct cell lines or distinct stimuli can be performed to validate the method's inference before its use *in vivo* and for generation counts beyond the range possible with division diluting dyes or fluorescence microscopy.

The construct described in this section is intended as an exemplar, creatable with present technology. Further experimental possibilities, including those based on naturally occurring mutations, can be found in the following Discussion.

8 Discussion

The estimators introduced in this article, eq. (1) and eq. (2), offer means to estimate a biologically significant quantity, the average generation of cell populations, for cell systems where direct measurement poses a significant challenge. Their appropriateness is not intuitively apparent and their development requires several mathematical results. Throughout the development of those results we assume that the label change is one-way, which can be shown not to be essential for the cumulant generating function derivation of the estimators, but is relied on in establishing the sample-path results as if the label change is reversible, so that labels can be gained as well as lost, then asymptotically it is known that the growth rate of the number of label-positive cells equals the growth rate of the total number of cells [43].

Despite its less than obvious genesis, the estimator has highly desirable features: it allows the population to be subject to death and division; it does not need to know the number of progenitors; it does not require knowledge of cell-cycle distributions; and, subject to knowing the per-division label-change probability, only requires the measurement of proportions. Comparison of estimates for simulations suggest that the estimator is accurate for physiological reasonable parameterizations.

The estimators (1) and (2) depend on the proportion of label-positive cells in the population, where the label can be any of the cell's properties that is lost with a small probability during its division cycle. Several naturally occurring and engineered cellular processes exist that approximately match this requirement. Somatic mutation is probably the best studied natural process of this kind. In this case germ-line cells are defined to be label-positive, while label-negative cells correspond to those with mutations in their DNA. The proportion of label-positive cells can be assessed by next generation sequencing. In humans there is a high rate of fidelity in DNA replication, giving an error rate of 5×10^{-11} per base per division [11] and so using only a single nucleotide location as a label appears impractical. Considering instead the full germ-line genome as a positive label, even though each nucleotide may suffer mutations with distinct rates, and potentially in concert, there is still an over-all probability of label-change that has been estimated in human sperm cells as approximately $p = 4 \times 10^{-3}$ [11]. In principle, this rate could be used as the probability of delabeling for our estimator. Alternatively, hotspots of mutation could also be analyzed. For example, micro-satellites, short repetitive sequences of DNA, mutate in humans with p in the range $(10^{-4}, 10^{-3})$, which we have used for the parameterization to evaluate the performance of our estimator.

The use of hotspots of mutation as a label suffers from the difficulty that delabeled cells could relabel due to the occurrence of further mutations. The impact of this can be ameliorated by creating an asymmetry in the likelihood of relabeling to delabeling. One selects a set of N sites for measurement, each having their own probability of mutation, p_i . One defines the label-positive cells as those that have germ-line values at all sites. The likelihood of a labeled cell delabeling is the likelihood that any of the sites mutate away from germ-line, $p = 1 - \prod_{i=1}^N (1 - p_i) \approx \sum_{i=1}^N p_i$, if the individual p_i are small. The likelihood that a cell with a single mutation relabels is $p_i \ll p$, creating a significant asymmetry. Moreover, for a cell that has had several mutations, the likelihood that all revert, which is necessary for relabeling, is smaller still.

While it seems likely that one must rely on naturally occurring processes to estimate the average generation of a cell population for humans, genetically modified cell lines and animals have the advantage that measuring the proportion of label-positive cells can be directly facilitated by fluorescent markers. The construct described in the Experiment Design section could be built or existing constructions, such as Cre-mediated sister chromatid recombination [65, 36, 73] and micro-satellite mutation induced label activation [59, 30], can be adapted, so that reversion does not occur. Using fluorescence-activated cell sorting or live imaging technologies and the estimators developed in this article it could be possible to follow the average generation of specific cell populations, like neoplastic tissue or the skin, in living organisms over long periods of time.

Recent evidence from *in vivo* cell lineage tracing techniques such as Cellular Barcoding [19] has demonstrated that apparently homogeneous progenitors give rise to heterogeneous families in cancer, immunology and hematopoiesis, e.g. [37, 34, 6, 17, 45]. Theoretical work developing methodologies to interrogate data from these experiments is ongoing, but one key difficulty that must be overcome is that the generation of individual families is unknown [47]. Combining any of the above experimental methodologies and using the estimator developed in the present article would allow inference of the per progenitor average generation, enhancing the deductive power of these techniques, which have already

proved invaluable. Having established the estimators and validating them through simulations and comparison with published data, we believe these are promising avenues.

Acknowledgments: The authors thank Søren Asmussen (Aarhus University) for drawing their attention to [2]. The work of T.W., L.P. and K.D. was supported by Human Frontier Science Program grant RGP0060/2012. K.D. was also supported by Science Foundation Ireland grant 12 IP 1263.

References

- [1] R. C Allsopp, H. Vaziri, C. Patterson, S. Goldstein, E. V. Younglai, A. B. Futcher, C. W. Greider, and C. B. Harley. Telomere length predicts replicative capacity of human fibroblasts. Proc. Natl. Acad. Sci. U.S.A., 89(21):10114–10118, 1992.
- [2] S. Asmussen. A probabilistic look at the Wiener-Hopf equation. SIAM Rev., 40(2):189–201, 1998.
- [3] K. B. Athreya and N. Kaplan. Convergence of the age distribution in the one-dimensional supercritical age-dependent branching process. Ann. Probability, 4(1):38–50, 1976.
- [4] L. Bai, G. Charvin, E. D. Siggia, and F. R. Cross. Nucleosome-depleted regions in cell-cycle-regulated promoters ensure reliable gene expression in every cell cycle. Dev. Cell, 18(4):544–555, April 2010.
- [5] R. Bellman and T. Harris. On age-dependent binary branching processes. Ann. of Math. (2), 55:280–295, 1952.
- [6] V. R. Buchholz, M. Flossdorf, I. Hensel, L. Kretschmer, B. Weissbrich, P. Gräf, A. Verschoor, M. Schiemann, T. Höfer, and D. H. Busch. Disparate individual fates compose robust CD8+ T cell immunity. Science, 340(6132):630–635, 2013.
- [7] A. Carlson, C. A .and Kas, R. Kirkwood, L. E. Hays, B. D. Preston, S. J. Salipante, and M. S. Horwitz. Decoding cell lineage from acquired mutations using arbitrary deep sequencing. Nat. methods, 9(1):78–80, 2012.
- [8] K. S. Crump and C. J. Mode. An age-dependent branching process with correlations among sister cells. J. Appl. Probability, 6(1):205–210, 1969.
- [9] R. J. De Boer and A. S. Perelson. Quantifying T lymphocyte turnover. J. Theor. Bio., 327:45–87, 2013.
- [10] M. R. Dowling, A. Kan, S. Heinzel, J. H. S. Zhou, J. M. Marchingo, C. J. Wellard, J. F. Markham, and P. D. Hodgkin. Stretched cell cycle model for proliferating lymphocytes. Proc. Natl. Acad. Sci. U.S.A., 111(17):6377–6382, 2014.
- [11] J. W. Drake, B. Charlesworth, D. Charlesworth, and J. F. Crow. Rates of spontaneous mutation. Genetics, 148(4):1667–1686, 1998.
- [12] K. R. Duffy and V. G. Subramanian. On the impact of correlation between collaterally consanguineous cells on lymphocyte population dynamics. J. Math. Biol., 59(2):255–285, 2009.

- [13] K. R. Duffy, C. J. Wellard, J. F. Markham, J. H. S. Zhou, R. Holmberg, E. D. Hawkins, J. Hasbold, M. R. Dowling, and P. D. Hodgkin. Activation-induced B cell fates are selected by intracellular stochastic competition. Science, 335(6066):338–341, 2012.
- [14] W. Feller. An introduction to probability theory and its applications. Vol. I. John Wiley & Sons Inc., 1968.
- [15] S. A. Frank, Y. Iwasa, and M. A. Nowak. Patterns of cell division and the risk of cancer. Genetics, 163(4):1527–1532, 2003.
- [16] C. Gasche, C. L. Chang, L. Natarajan, A. Goel, J. Rhees, D. J. Young, C. N. Arnold, and C. R. Boland. Identification of frame-shift intermediate mutant cells. Proc. Natl. Acad. Sci. U.S.A., 100(4):1914–1919, 2003.
- [17] C. Gerlach, J. C. Rohr, L. Perié, N. van Rooij, J. W. J. van Heijst, A. Velds, J. Urbanus, S. H. Naik, H. Jacobs, J. B. Beltman, R. de Boer, and T. Schumacher. Heterogeneous differentiation patterns of individual CD8+ T cells. Science, 340(6132):635–639, 2013.
- [18] C. A. Giurumescu, S. Kang, T. A. Planchon, E. Betzig, J. Bloomekatz, D. Yelon, P. Cosman, and A. D. Chisholm. Quantitative semi-automated analysis of morphogenesis with single-cell resolution in complex embryos. Development, 139(22):4271–4279, 2012.
- [19] J. A. Golden, S. C. Fields-Berry, and C. L. Cepko. Construction and characterization of a highly complex retroviral library for lineage analysis. Proc. Natl. Acad. Sci. U.S.A., 92(12):5704–5708, 1995.
- [20] F. L. Gomes, G. Zhang, F. Carbonell, J. A. Correa, W. A. Harris, B. D. Simons, and M. Cayouette. Reconstruction of rat retinal progenitor cell lineages in vitro reveals a surprising degree of stochasticity in cell fate decisions. Development, 138(2):227–235, 2011.
- [21] C. B. Harley, A. B. Futcher, and C. W. Greider. Telomeres shorten during ageing of human fibroblasts. Nat. Genet., 345(6274):458–460, 1990.
- [22] T. E. Harris. The theory of branching processes. Springer-Verlag, Berlin, 1963.
- [23] E. D. Hawkins, M. Hommel, M. L. Turner, F. L. Battye, J. F. Markham, and P. D. Hodgkin. Measuring lymphocyte proliferation, survival and differentiation using CFSE time-series data. Nat. Protoc., 2(9):2057–2067, 2007.
- [24] E. D. Hawkins, J. F. Markham, L. P. McGuinness, and P. D. Hodgkin. A single-cell pedigree analysis of alternative stochastic lymphocyte fates. Proc. Natl. Acad. Sci. U.S.A., 106(32):13457–13462, 2009.
- [25] M. Hills, K. Lücke, E. A. Chavez, C. J. Eaves, and P. M. Lansdorp. Probing the mitotic history and developmental stage of hematopoietic cells using single telomere length analysis (STELA). Blood, 113(23):5765–5775, 2009.
- [26] P. Jagers. The proportions of individuals of different kinds in two-type populations. A branching process problem arising in biology. J. Appl. Probability, 6:249–260, 1969.
- [27] P. Jagers. Renewal theory and the almost sure convergence of branching processes. Arkiv för Matematik, 7(6):495–504, 1969.

- [28] L. Kaszubowska. Telomere shortening and ageing of the immune system. J. Physiol. Pharmacol., 59:169–186, 2008.
- [29] M. Kimmel and D. E. Axelrod. Branching Processes in Biology. Springer, 2002.
- [30] W. Koole, H. S. Schäfer, R. Agami, G. van Haaften, and M. Tijsterman. A versatile microsatellite instability reporter system in human cells. Nucleic Acids Res., 41(16):e158, 2013.
- [31] W. Koole and M. Tijsterman. Mosaic analysis and tumor induction in zebrafish by microsatellite instability-mediated stochastic gene expression. Dis. Model Mech., 7(7):929–936, July 2014.
- [32] S. Kozar, E. Morrissey, A. M. Nicholson, M. van der Heijden, H. I. Zecchini, R. Kemp, S. Tavaré, L. Vermeulen, and D. J. Winton. Continuous clonal labeling reveals small numbers of functional stem cells in intestinal crypts and adenomas. Cell Stem Cell, 13(5):626–633, November 2013.
- [33] S. G. Krantz and H. R. Parks. A primer of real analytic functions. Birkhäuser Boston, 2002.
- [34] A. Kreso, C. A. O’Brien, P. van Galen, O. I. Gan, F. Notta, A. M. K. Brown, K. Ng, J. Ma, E. Wienholds, C. Dunant, A. Pollett, S. Gallinger, J. McPherson, C. G. Mullighan, D. Shibata, and J. E. Dick. Variable clonal repopulation dynamics influence chemotherapy response in colorectal cancer. Science, 339(6119):543–548, 2013.
- [35] N. Levinson. Limiting theorems for age-dependent branching processes. Illinois J. Math., 4:100–118, 1960.
- [36] C. Liu, J. C. Sage, M. R. Miller, R. G. Verhaak, S. Hippenmeyer, H. Vogel, O. Foreman, R. T. Bronson, A. Nishiyama, L. Luo, and H. Zong. Mosaic analysis with double markers reveals tumor cell of origin in glioma. Cell, 146(2):209–221, July 2011.
- [37] R. Lu, N. F. Neff, S. R. Quake, and I. L. Weissman. Tracking single hematopoietic stem cells in vivo using high-throughput sequencing in conjunction with viral genetic barcoding. Nat. Biotechnol., 29(10):928–933, 2011.
- [38] A. B. Lyons. Analysing cell division in vivo and in vitro using flow cytometric measurement of CFSE dye dilution. J. Immunol. Methods, 243(1):147–154, 2000.
- [39] A. B. Lyons and C. R. Parish. Determination of lymphocyte division by flow cytometry. J. Immunol. Methods, 171(1):131–137, 1994.
- [40] J. M. Marchingo, A. Kan, R. M. Sutherland, K. R. Duffy, C. J. Wellard, G. T. Belz, A. M. Lew, M. R. Dowling, S. Heinzel, and P. D. Hodgkin. Antigen affinity, costimulation, and cytokine inputs sum linearly to amplify T cell expansion. Science, 346(6213):1123–1127, 2014.
- [41] J. F. Markham, C. J. Wellard, E. D. Hawkins, K. R. Duffy, and P. D. Hodgkin. A minimum of two distinct heritable factors are required to explain correlation structures in proliferating lymphocytes. J. R. Soc. Interface, 7(48):1049–1059, 2010.
- [42] L. M. F. Merlo, J. W. Pepper, B. J. Reid, and C. C. Maley. Cancer as an evolutionary and ecological process. Nat. Rev. Cancer, 6(12):924–935, 2006.
- [43] C. J. Mode. Restricted transition probabilities and their applications to some problems in the dynamics of biological populations. Bull. Math. Biophys., 28:315–331, 1966.

- [44] A. Nagy. Cre recombinase: the universal reagent for genome tailoring. *Genesis*, 26:99–109, 2000.
- [45] S. Naik, L. Perié, E. Swart, C. Gerlach, N. van Rooi, R. de Boer, and T. Schumacher. Diverse and heritable lineage imprinting of early haematopoietic progenitors. *Nature*, 496:229–233, 2013.
- [46] P. Olofsson. Branching processes with local dependencies. *Ann. Appl. Probab.*, 6(1):238–268, 1996.
- [47] L. Perié, P. D. Hodgkin, S. H. Naik, T. N. Schumacher, R. J. de Boer, and K. R. Duffy. Determining lineage pathways from cellular barcoding experiments. *Cell Rep.*, 6(4):617–624, 2014.
- [48] E. O. Powell. Some features of the generation times of individual bacteria. *Biometrika*, 42:16–44, 1955.
- [49] B. J. C. Quah and C. R. Parish. New and improved methods for measuring lymphocyte proliferation in vitro and in vivo using CFSE-like fluorescent dyes. *J. Immunol. Methods*, 379(1):1–14, 2012.
- [50] Y. Reizel, N. Chapal-Ilani, R. Adar, S. Itzkovitz, J. Elbaz, Y. E. Maruvka, E. Segev, L. I. Shlush, N. Dekel, and E. Shapiro. Colon stem cell and crypt dynamics exposed by cell lineage reconstruction. *PLoS genetics*, 7(7):e1002192, 2011.
- [51] S. I. Resnick. *Adventures in Stochastic Processes*. Birkhäuser Boston, 1992.
- [52] J. L. Richards, A. L. Zacharias, T. Walton, J. T. Burdick, and J. I. Murray. A quantitative model of normal caenorhabditis elegans embryogenesis and its disruption after stress. *Dev. Biol.*, 374(1):12–23, 2013.
- [53] N. Rufer, T. H. Brümmendorf, S. Kolvraa, C. Bischoff, K. Christensen, L. Wadsworth, M. Schulzer, and P. M. Lansdorp. Telomere fluorescence measurements in granulocytes and T lymphocyte subsets point to a high turnover of hematopoietic stem cells and memory T cells in early childhood. *J. Exp. Med.*, 190(2):157–168, 1999.
- [54] A. Sakaue-Sawano, H. Kurokawa, T. Morimura, A. Hanyu, H. Hama, H. Osawa, S. Kashiwagi, K. Fukami, T. Miyata, H. Miyoshi, T. Imamura, M. Ogawa, H. Masai, and A. Miyawaki. Visualizing spatiotemporal dynamics of multicellular cell-cycle progression. *Cell*, 132(3):487–498, 2008.
- [55] M. L. Samuels. Distribution of the branching-process population among generations. *J. Appl. Probability*, 8:655–667, 1971.
- [56] R. J. Serfling. *Approximation Theorems of Mathematical Statistics*. Wiley, New York, 1980.
- [57] D. Shibata, W. Navidi, R. Salovaara, Z.-H. Li, and L. A. Aaltonen. Somatic microsatellite mutations as molecular tumor clocks. *Nat. Med.*, 2(6):676–681, 1996.
- [58] D. Shibata and S. Tavaré. Counting divisions in a human somatic cell tree. *Cell Cycle*, 5(6):610–614, 2006.
- [59] R. J. C. Slebos, D. S. Oh, D. M. Umbach, and J. A. Taylor. Mutations in Tetranucleotide Repeats following DNA Damage Depend on Repeat Sequence and Carcinogenic Agent. *Cancer Res.*, 62(21):6052–6060, November 2002.

- [60] J. A. Smith and L. Martin. Do cells cycle? Proc. Natl. Acad. Sci. U.S.A., 70(4):1263–1267, 1973.
- [61] H. J. Snippert, L. G. van der Flier, T. Sato, J. H. van Es, M. van den Born, C. Kroon-Veenboer, N. Barker, A.M. Klein, J. van Rheenen, B. D. Simons, and H. Clevers. Intestinal crypt homeostasis results from neutral competition between symmetrically dividing Lgr5 stem cells. Cell, 143(1):134–144, 2010.
- [62] A. Stuart and J. K. Ord. Kendall’s advanced theory of statistics. Vol. 1. Edward Arnold, London, 1994.
- [63] J. E. Sulston, E. Schierenberg, J. G. White, and J. N. Thomson. The embryonic cell lineage of the nematode *Caenorhabditis elegans*. Dev. Biol., 100(1):64–119, 1983.
- [64] J. X. Sun, A. Helgason, G. Masson, S. S. Ebenesersdottir, H. Li, S. Mallick, S. Gnerre, N. Patterson, A. Kong, D. Reich, and K. Stefansson. A direct characterization of human mutation based on microsatellites. Nat. Genet., 44(10):1161–1165, 2012.
- [65] L. Sun, X. Wu, M. Han, T. Xu, and Y. Zhuang. A mitotic recombination system for mouse chromosome 17. Proc. Natl. Acad. Sci. U.S.A., 105(11):4237–4241, 2008.
- [66] C. Tomasetti and B. Vogelstein. Variation in cancer risk among tissues can be explained by the number of stem cell divisions. Science, 347(6217):78–81, 2015.
- [67] J.-L. Tsao, Y. Yatabe, R. Salovaara, H. J. Järvinen, J.-P. Mecklin, L. A. Aaltonen, S. Tavaré, and D. Shibata. Genetic reconstruction of individual colorectal tumor histories. Proc. Natl. Acad. Sci. U.S.A., 97(3):1236–1241, 2000.
- [68] H. Vaziri, W. Dragowska, R. C. Allsopp, T. E. Thomas, C. B. Harley, and P. M. Lansdorp. Evidence for a mitotic clock in human hematopoietic stem cells: loss of telomeric DNA with age. Proc. Natl. Acad. Sci. U.S.A., 91(21):9857–9860, 1994.
- [69] H. Vaziri, F. Schächter, I. Uchida, L. Wei, X. Zhu, R. Effros, D. Cohen, and C. B. Harley. Loss of telomeric DNA during aging of normal and trisomy 21 human lymphocytes. Am. J. Hum. Genet., 52(4):661–667, 1993.
- [70] A. Wasserstrom, D. Frumkin, R. Adar, S. Itzkovitz, T. Stern, S. Kaplan, G. Shefer, I. Shur, L. Zangi, Y. Reizel, A. Harmelin, Y. Dor, N. Dekel, Y. Reisner, D. Benayahu, E. Tzahor, E. Segal, and E. Y. Shapiro. Estimating cell depth from somatic mutations. PLoS Comput. Biol., 4(5), 2008.
- [71] T. S. Weber, I. Jaehnert, C. Schichor, M. Or-Guil, and J. Carneiro. Quantifying the length and variance of the eukaryotic cell cycle phases by a stochastic model and dual nucleoside pulse labelling. Plos Comput Biol, 10(7), July 2014.
- [72] S. L. Weinrich, R. Pruzan, L. Ma, M. Ouellette, V. M. Tesmer, S. E. Holt, A. G. Bodnar, S. Lichtsteiner, N. W. Kim, J. B. Trager, R. D. Taylor, R. Carlos, W. H. Andrews, W. E. Wright, J. W. Shay, C. B. Harley, and G. B. Morin. Reconstitution of human telomerase with the template RNA component hTR and the catalytic protein subunit hTRT. Nat. Genet., 17(4):498–502, 1997.
- [73] B. Zhang, M. Dai, Q.-J. Li, and Y. Zhuang. Tracking proliferative history in lymphocyte development with cre-mediated sister chromatid recombination. PLoS Genet., 9(10):e1003887, 10 2013.

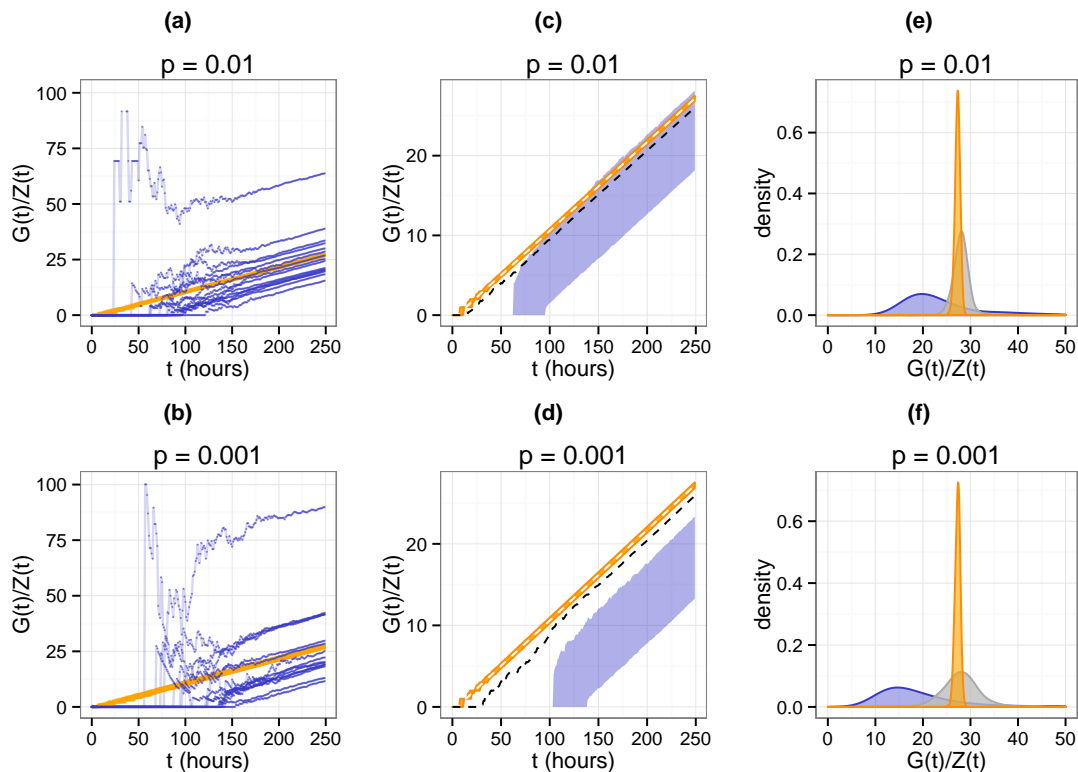


Figure 1: **Single progenitor simulation validation.** Simulations, described in detail in Section 5, start with a single label-positive cell at time 0. Plots shown for two label-change probabilities, $p = 10^{-2}$ (top row) and $p = 10^{-3}$ (bottom row). For 15 independent realizations, orange lines display the actual average generation, $G(t)/Z(t)$. Blue lines display the estimates $-1/p \log(Z^+(t)/Z(t))$ from (1), which ultimately increase linearly with the same slope as the average generation, but initially show significant variability. (c)-(d) For 100 independent realizations of the process, the dashed line reveals that the empirical average of the estimates is close to the true value. The blue region is an inter-quartile plot of the $-1/p \log(Z^+(t)/Z(t))$ estimates, with the upper boundary being where 25 of the realizations are larger and the lower boundary being where 25 of realizations are smaller, which typically exhibits under-estimation. (e)-(f) Using Monte Carlo methods and a standard kernel estimator, these panels show, for $t_2 = 250$ hours, the density of observations of $G(t_2)/Z(t_2)$ in orange, the single time-point estimate $-1/p \log(Z^+(t_2)/Z(t_2))$ in blue, and the two time-point estimate (2) in grey with an additional time point at $t_1 = 200$ hours. The additional time-point improves the estimate by removing early variability on a realization-by-realization basis.

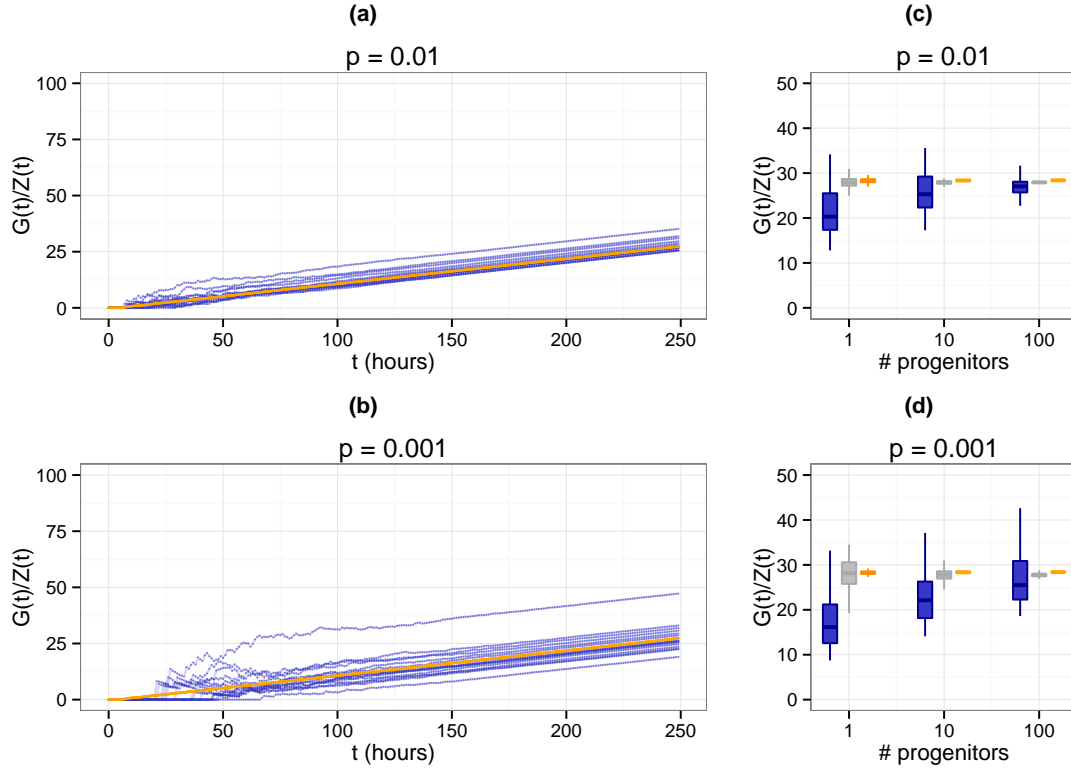


Figure 2: **Multiple progenitor in silico validation.** Plots shown for two label-change probabilities, $p = 10^{-2}$ (top row) and $p = 10^{-3}$ (bottom row). (a)-(b) Sample paths of 15 independent realizations with 100 progenitors. Orange lines correspond to average generation, $G(t)/Z(t)$. Blue lines display the estimates $-1/p \log(Z^+(t)/Z(t))$, whose early time fluctuation is significantly less pronounced than with a single progenitor, as in Fig. 1 (a)-(b). (c)-(d) For 1, 10 and 100 progenitors, Monte Carlo generated box plots of average generation (orange) and single time-point estimates (blue) at $t = 250$ hours, and two time-point estimates (grey), with the additional measurement at $t_1 = 200$ hours. As predicted by theory, accuracy improves substantially, in a p dependent fashion, as the number of progenitors increases.

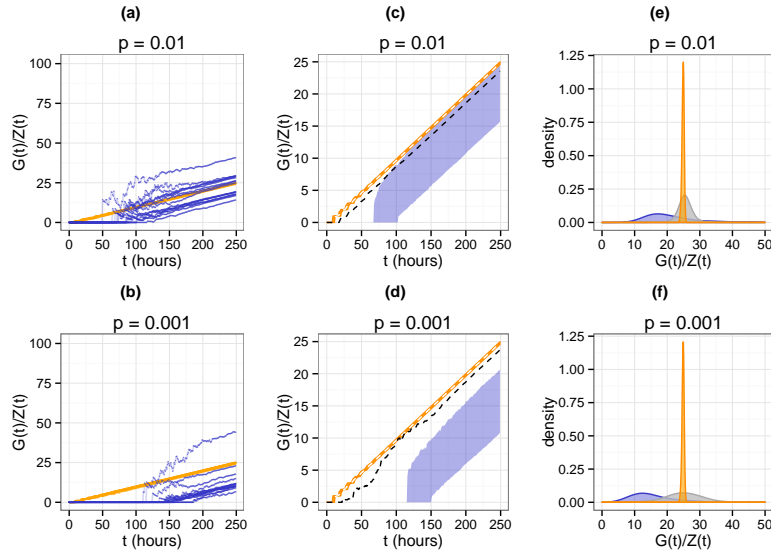


Figure 3: Similar results to those shown in Fig. 1, but using a cell life-time distributed according to a delayed Gamma distribution with shape parameter of 3, scale parameter of 1 and a delay of 7 hours.

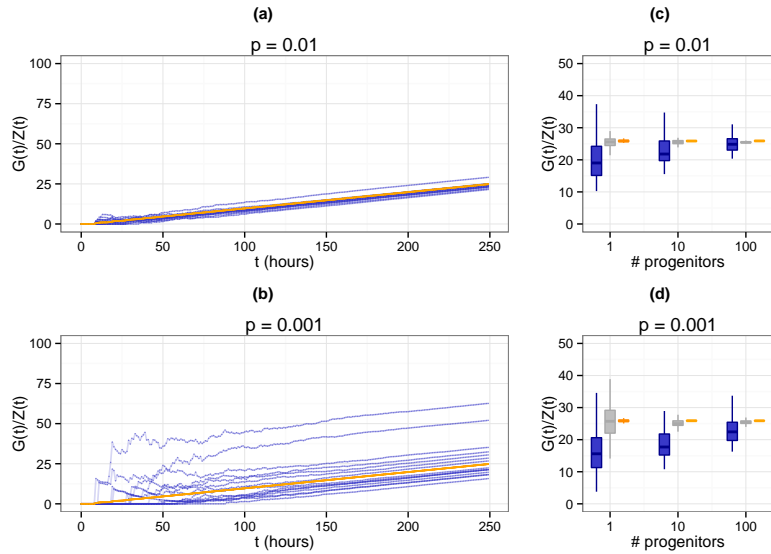


Figure 4: Similar results to those shown in Fig. 2, but using a cell life-time distributed according to a delayed Gamma distribution with shape parameter of 3, scale parameter of 1 and a delay of 7 hours.

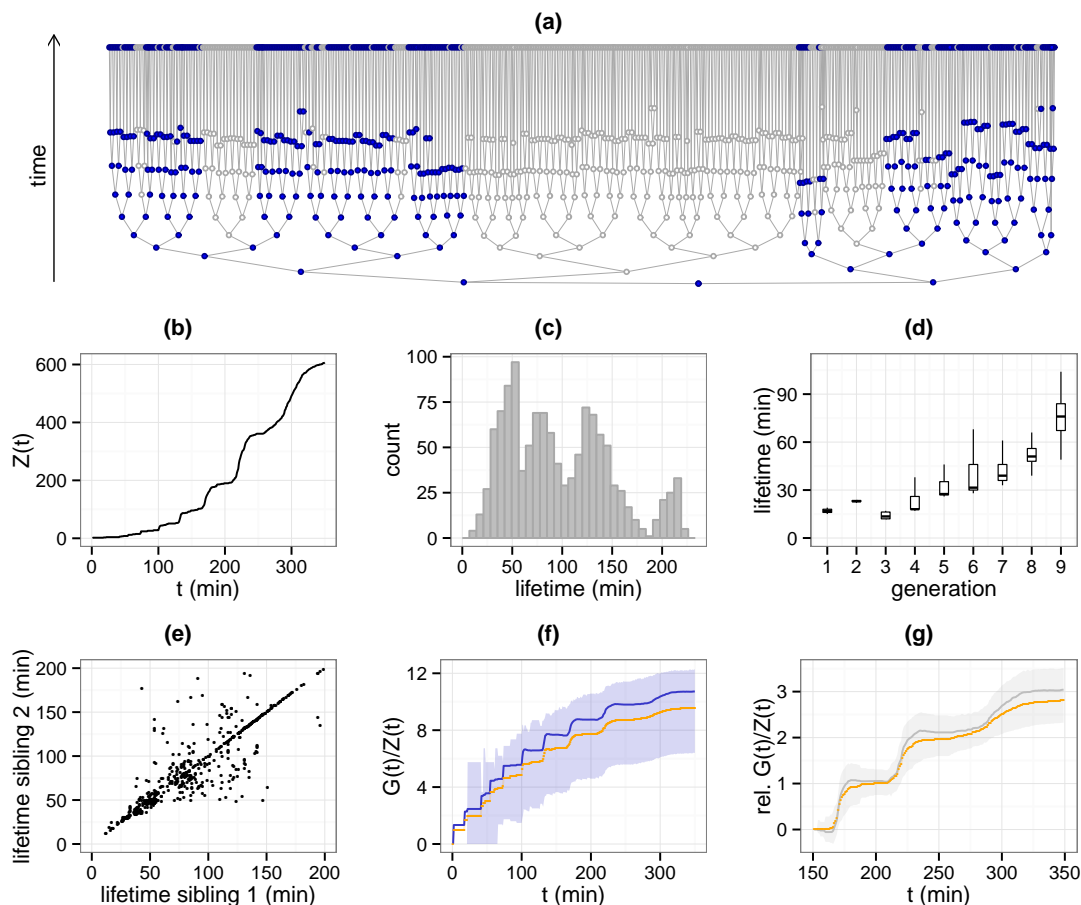


Figure 5: **Validation with data from time-lapse microscopy.** *C. elegans* embryonic development tree taken from three-dimensional time-lapse movies of embryos recorded over approximately six hours, supplementary material of [52], and decorated with a stochastic labeling with $p = 0.05$. (a) Lineage tree of *C. elegans* embryos, for first nine generations. The lowest node represents the progenitor present in the first frame, while the uppermost nodes represent cells alive in the last frame. Each node in between represents a division event, and its vertical position corresponds to the frame in which it was recorded. The color of the nodes, blue for label-positive at division and white for label-negative at division, illustrate one possible random delabeling of the trees. (b) Total population, $Z(t)$, as a function of time, t , shows a step-wise increase in cell numbers followed by a reduction in growth rate that is not consistent with a homogeneous age dependent branching process. (c) Histogram of the cell lifetime shows a multi-modal distribution, partly explained by the fact that lifetimes appear to lengthen with time of birth or generation. (d) Box plot of the lifetimes as a function of generation, which shows lifetimes increasing with generation. (e) Sibling lifetimes are highly correlated, with many dividing during the same frame. (f) Comparison of average generation $G(t)/Z(t)$ (orange) with its estimate $-\log(Z^+(t)/Z(t))/p$ (blue). Monte Carlo determined inter-quartile ranges based on 10^4 samples. (g) Same as (f), but starting at $t_1 = 150$ and computing the difference of the average generation $G(t)/Z(t)$ (orange) since t_1 via the approximation (2).

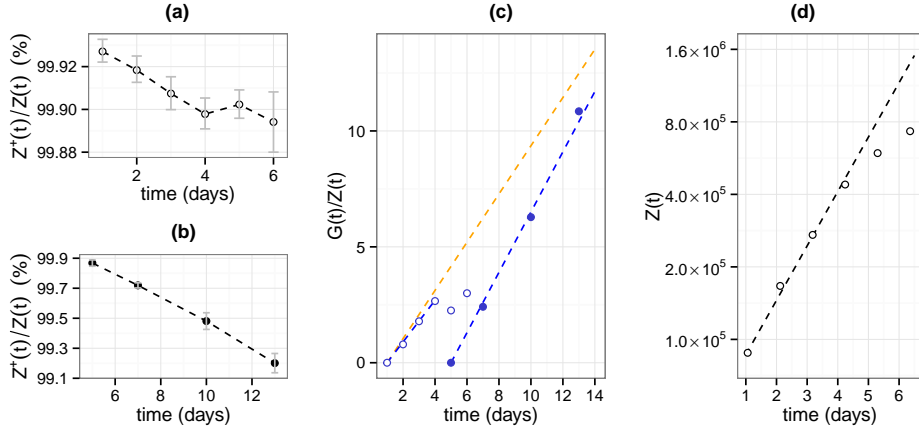


Figure 6: **Validation with data from micro-satellite reporter systems.** (a-b) Percentage of unlabeled cells $Z^+(t)/Z(t)$ over several days of culture for genetically modified clones of MEF cells (a, [32]) and HCT116 cells (b, [16]) carrying micro-satellite mutation reporter cassettes. The mutation probabilities, as reported in the respective studies are 1.1×10^{-4} [32] and 6.1×10^{-4} [16], which we use for p , the probability of delabeling per cell division. Data are represented as mean \pm SEM. For the HCT116 data, the mean at each time point is over three clones. (c) Inferred relative average generation $G(t)/Z(t)$ from the proportions of unlabeled cells and p using the estimator $1/p \log(Z^+(t)/Z(t))$ (MEF, open circles; HCT116, filled circles). For both data sets the average generation increases linearly with time, as expected from the theory. In addition, the slope is close to one generation per day, even though the mutation probability p differs by a factor of six. The orange dashed line shows the increase in average generation as estimated directly from the growth curve $Z(t)$ (panel d) assuming exponentially distributed life-times and no cell death (for details see main text), demonstrating the accuracy of the estimator. The blue dashed regression lines ($r^2 = 0.99$ for both sets) highlight the linear increase of average generation estimates during the exponential growth phase. (d) Population size $Z(t)$ of cultured MEF cells (open circles, [32]) and exponential growth fit to first four time points (dashed line, $r^2 = 0.97$).

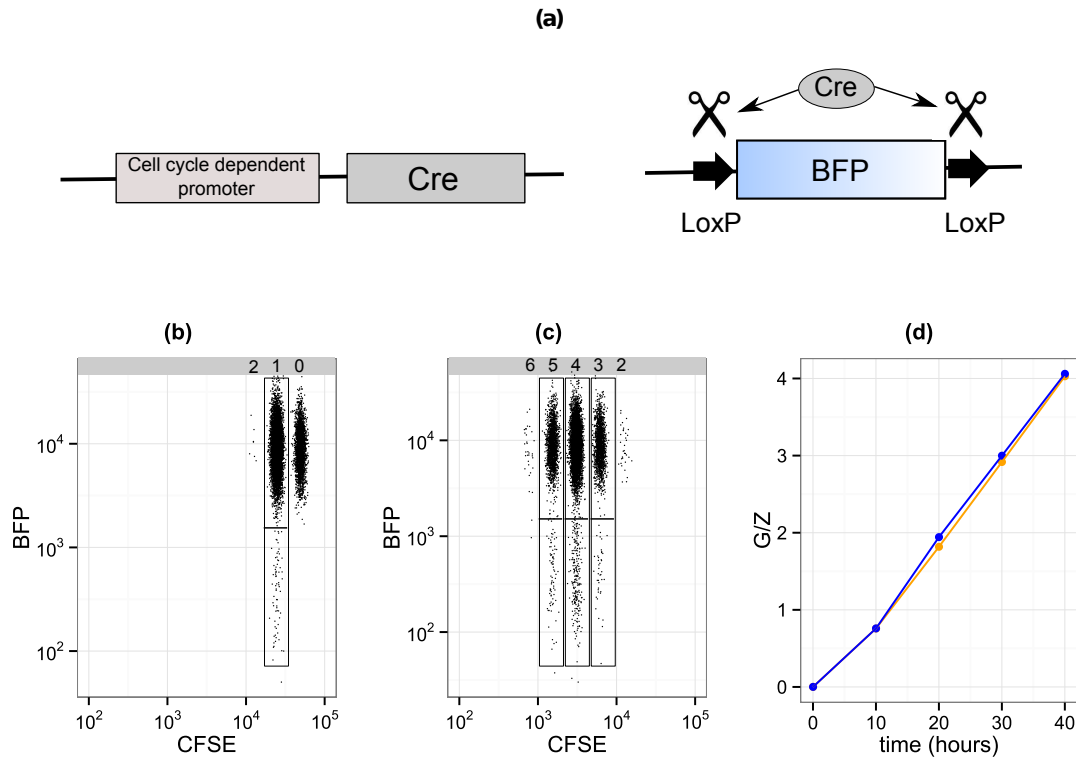


Figure 7: **Proposed probabilistic division-linked label-loss construct.** (a) Schematic drawing of the construct. Cells initially express a protein such as Blue Fluorescent Protein (BFP). During each cell cycle Cre is expressed and with a small probability the gene for BFP is excised, leading to irreversible label-loss. (b)-(d) In silico simulation of proposed FACS experiment to determine the probability of label-loss, p . The simulation is parameterized as in Section 5. 20,000 BFP+ cells are labeled with a division diluting dye such as CFSE, which is green, and cultured until they divide. At each division, CFSE is shared evenly between daughters and the BFP label is lost with probability $p = 0.01$. (b)-(c) Simulated FACS plots, ten and 40 hours after CFSE labeling. The fluorescence signals were set to realistic experimental values [23] and noise was added to initial CFSE levels for illustrative purposes. The gates in (b) and (c) capture the proportion of label-positive cells, $BFP^+(n)$, in each generation, n . From these, the label-loss probability, p , can be experimentally determined via the formula $p = 1 - BFP^+(n+1)/BFP^+(n)$. As all cells in the zeroth generation express BFP, $BFP^+(0) = 1$, and so $p = 1 - BFP^+(1) = BFP^-(1) = 0.0101$, the proportion of BFP negative cells in generation 1. (d) The orange line plots the average generation of the population, determined from the simulated CFSE data, a function of time. The blue line is estimate determined using the method described in the present paper (1) with a label-loss parameter, $p = 0.0101$, obtained from (b). The CFSE determined value and the estimate exhibit excellent concordance.